NASA CR-54869

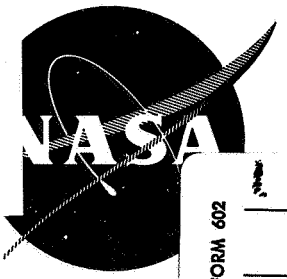

THIOKOL 260-SL SUBSCALE NOZZLE VERIFICATION PROGRAM

prepared for

NATIONAL AERONAUTICS AND SPACE ADMINISTRATION

CONTRACT NAS 3-6285

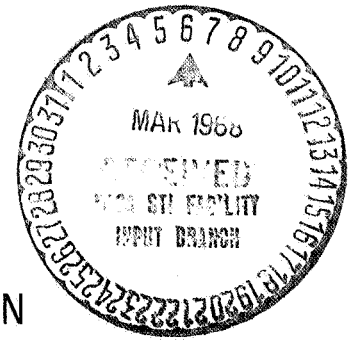

THIOKOL CHEMICAL CORPORATION

Space Booster Division

Brunswick, Georgia

CR-54869

SUBSCALE NOZZLE VERIFICATION PROGRAM;

65-SS-2 AND 65-SS-3 MOTORS

18 JAN 1966

Prepared Under Contract No. NAS 3-6285 By
THIOKOL CHEMICAL CORPORATION
Space Booster Division
Brunswick, Georgia

for Lewis Research Center

NATIONAL AERONAUTICS AND SPACE ADMINISTRATION

Requests for copies of this report should be referred to

National Aeronautics and Space Administration
Office of Scientific and Technical Information
Attention: AFSS-A
Washington, D.C. 20546

TABLE OF CONTENTS

LIST OF ILLUSTRATIONS

LIST OF ILLUSTRATIONS
(Cont'd.)

LIST OF TABLES

I. SUMMARY AND CONCLUSION

The successful static test of the 65-SS-2 rocket motor demonstrated the acceptability of the basic nozzle design, the nozzle materials, and the ablative tape fabrication concepts which had been used in the design of the nozzles for the 156- and 260-inch rocket motors. Even though several of the bias tape components for this nozzle could not be wrapped by the techniques planned for the large nozzle because of their tape width to radius ratio, the fabrication of this nozzle did result in the solving of some of the ablative tape handling, heating, cooling, and curing problems. Several of the problems associated with the ablative raw materials were solved during the nozzle fabrication. Static testing of the nozzle subjected the ablative materials to Mach numbers closely approaching the flow condition they would encounter in the large nozzle.

Other program items verified by this motor test were the TP-H8163 propellant, TI-H704B case insulation, TA-G701B flap filler material, and the TI-H714A liner, all of which had been developed for the 156-2C-1 and 260-SL-1 motors. The entrance section of the nozzle was also used to test varying thicknesses of V-44 insulation and V-61 joint filler, which were scheduled for use in the adapter section of the 260-SL-1 motor. The referenced specific impulse of the propellant was calculated to have a value of 244.8 lb-sec/lb.

The successful performance of the 65-SS-3 motor reconfirmed the adequacy of the ablative insulation materials, fabrication processes for the nozzle, propellant, liner, and case insulation, as well as proved that the changes which had been made in the nozzle design based on the 65-SS-2 motor performance were satisfactory. The 65-SS-3 nozzle test provided data concerning an ambient cure tie laminate, which was added to alleviate fabrication problems, and, in addition, provided a test of TI-H704B insulation in an erosive environment. Ohio Rubber's ORCO-9250 which was being considered for use as the 260-SL-1 adapter insulation also performed satisfactorily. The 65-SS-3 motor also verified bonding of liner to propellant after a seven-day liner cure.

Significant program items verified by the testing of the two motors were the nozzle fabrication techniques, nozzle materials, liner material, and the propellant. All of these items were being developed for the 156-2C-1 and 260-SL-1 motors. Fabrication of the ablatives for the two nozzles provided information concerning the tooling required for ablative fabrication. This information was utilized in the design of the 156- and 260-inch tooling.

II. PROGRAM OBJECTIVES

The original scope of the 65-inch diameter motor subscale test program was to evaluate nozzle ablative materials and fabrication techniques, and obtain material loss rate data for the 156-2C-1 and 260-SL nozzle design. Specifically, nozzle design information was required on: (1) char and erosion rates of carbon cloth-phenolic, graphite cloth-phenolic, silica cloth-phenolic, and glass cloth-phenolic; (2) joint design and filler materials; (3) structural adequacy of glass overwrap and thermal expansion of mating ablative components; (4) adequacy of the adhesive bond between the steel shell and ablative nozzle components; and (5) verification of the structural tie laminate concept.

As the program progressed, changes in the original objectives were found to be necessary. During fabrication of the first subscale nozzle, it was determined that the tape widths required for the larger nozzles could not be successfully tape wrapped on the smaller subscale diameters. The ratio of tape width to mandrel radius, w/r, was excessive on some of the components resulting in extreme tape wrinkling and neckdown. The original objective of tape wrapping the subscale components was then modified to allow the hand layup technique to be utilized on all components which could not be tape wrapped.

In an effort to reduce costs on the program, several areas were investigated for possible changes. One of the first changes made affected the nozzle adapter for the 260-SL motors. A more economical method of insulating the adapter, other than using a tape wrapped component, was investigated. Initially, V-44 Buna-N material appeared to fulfill this objective. In order to demonstrate the acceptability of the V-44 material, varying thicknesses were applied over the tape wrapped phenolic impregnated carbon fabric utilized in the entrance cone of the first subscale nozzle. Results of the static test proved the material to be satisfactory.

The Thiokol mastic insulation material (TI-H704B), which was being developed for use in insulating the 156-2C-1 and 260-SL-1 cases proved to be lower in cost than the V-44 Buna-N material Therefore, the carbon entrance cone was completely deleted in the second subscale nozzle and was replaced by two 180-degree segments, one of mastic insulation and the other of V-44 insulation. The results of this test showed the mastic insulation to be completely satisfactory at Mach numbers below approximately 0.12.

In a further effort to reduce program costs, the third and fourth subscale nozzles were deleted, and the objective of fabricating a 260-SL-2 exit cone utilizing a nonhydroclave process was dropped from the program.

III. MOTOR CONFIGURATION

A. MOTOR 65-SS-1

The 65-SS-1 (TU-405) motor was designed by Thiokol's Wasatch Division as a subscale nozzle test motor. The design, shown in Figure 1, consisted of a shortened 1400 series heavyweight MINUTEMAN case, a special 65-inch diameter closure, cured-in-place Buna-N insulation, a thin layer of UF-2122 liner, and a slow burning propellant (TP-H1061). The grain design was a cylindrical port with a 23-inch web and 120-second burning time.

The loaded case was X-rayed and tangential shots indicated that there were separations between the propellant and insulation at the forward and aft head flaps, and smaller continuous separations along the length of the case sidewall. Propellant and insulation were removed and the case was degreased, grit blasted, preserved, and stored.

B. MOTORS 65-SS-2 and -3

The 65-SS-2 (TU-418.01) and 65-SS-3 (TU-418.02) motors were identical except for the nozzle assembly. After the bond failure in the 65-SS-1 motor, the objectives of the subscale program were expanded to include the demonstration of the insulation (TI-H704B), liner (TL-H704A), flap and flap filler (TA-G701B) material, and TP-H8163 propellant that were to be utilized in the 156-2C-1 and 260-SL motors. With this propellant the nominal web time is approximately 50 seconds. The motor cross section is shown in Figure 2, and Figure 3 depicts the grain configuration. Table I is the master drawing list for the 65-SS-2 and 65-SS-3 motors.

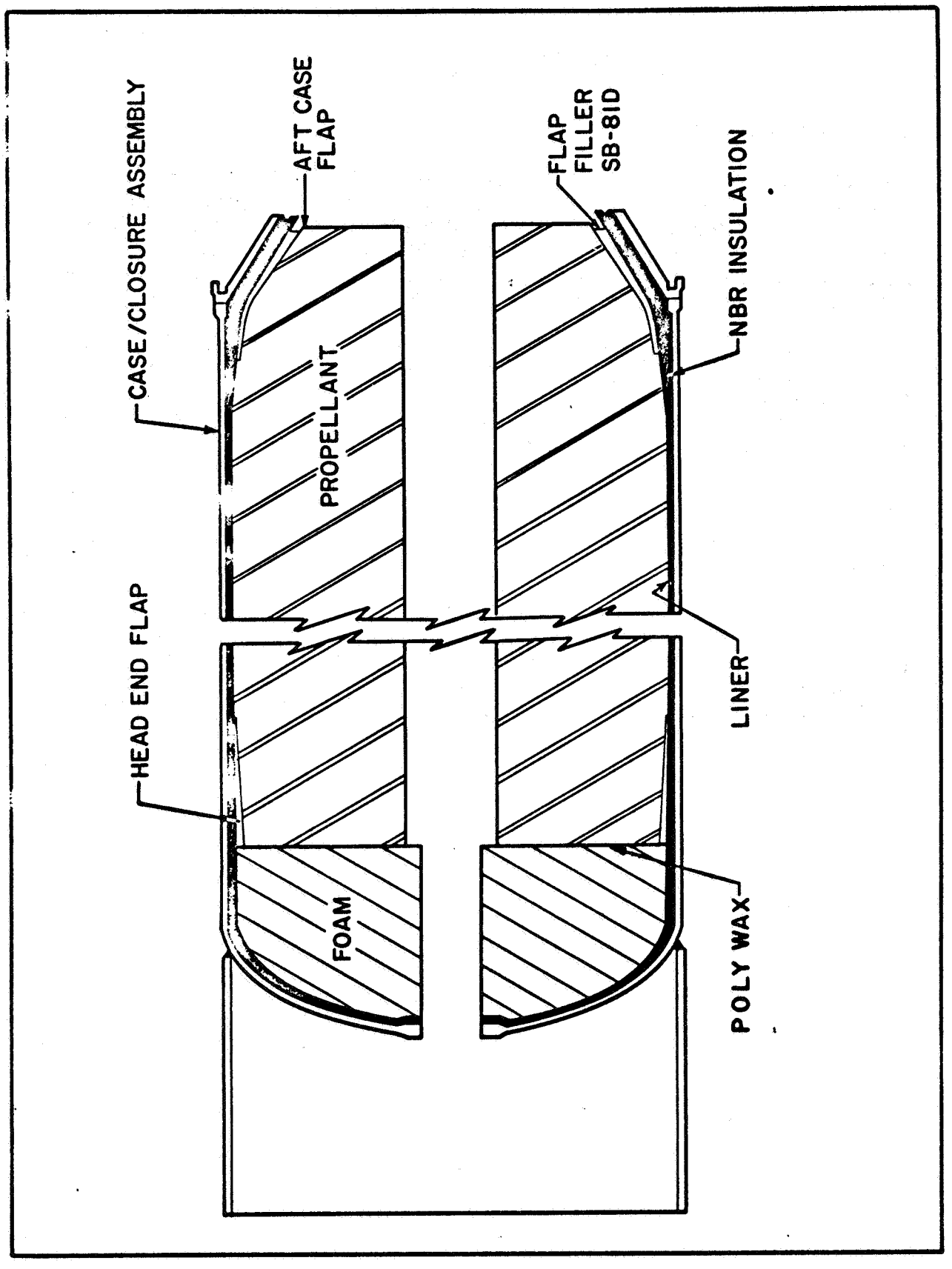

Figure 1 - Sectional View of the 65-SS-1 Static Test Motor

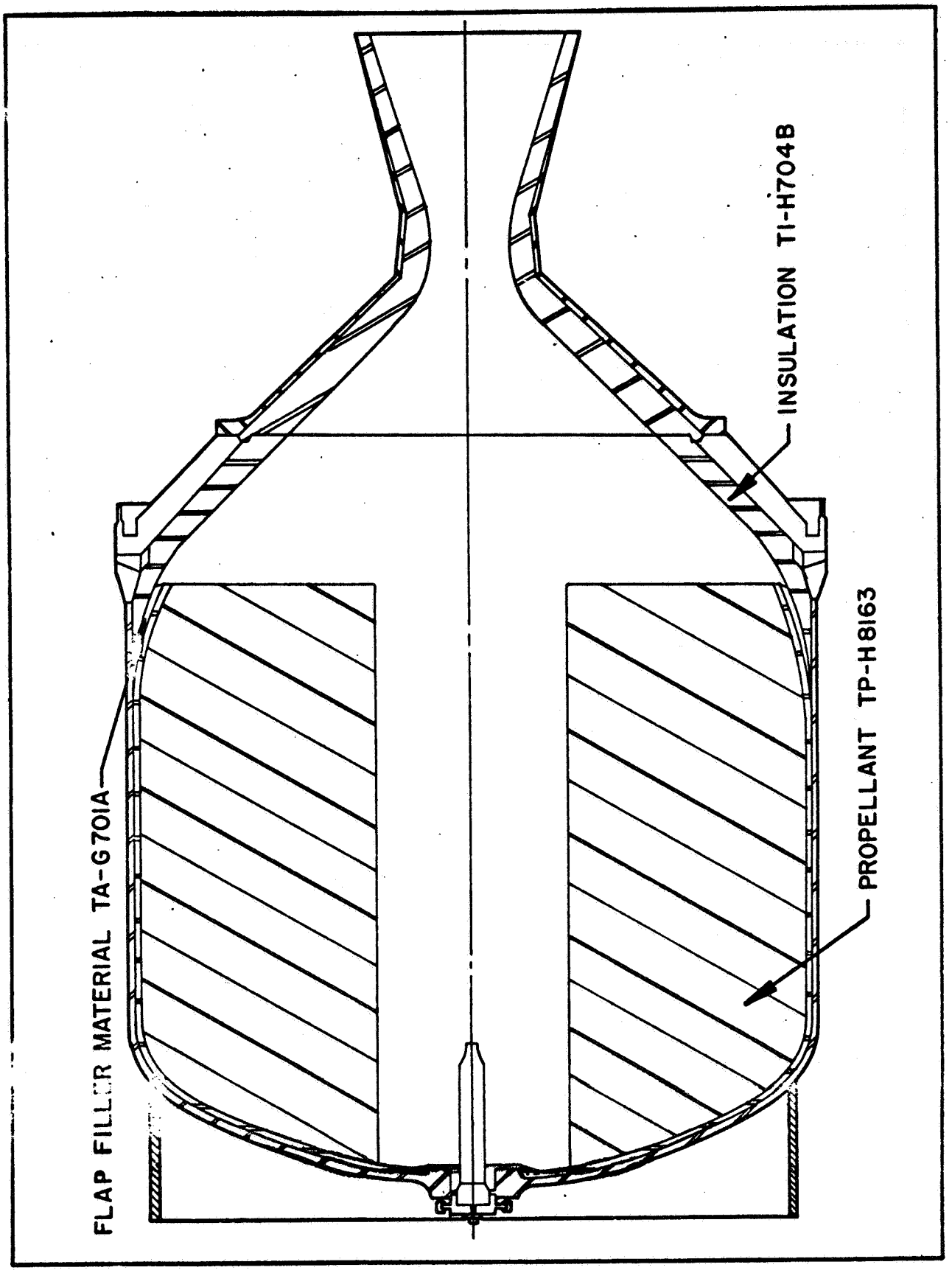

Figure 2 - Sectional View of the 65-SS-3 Static Test Motor

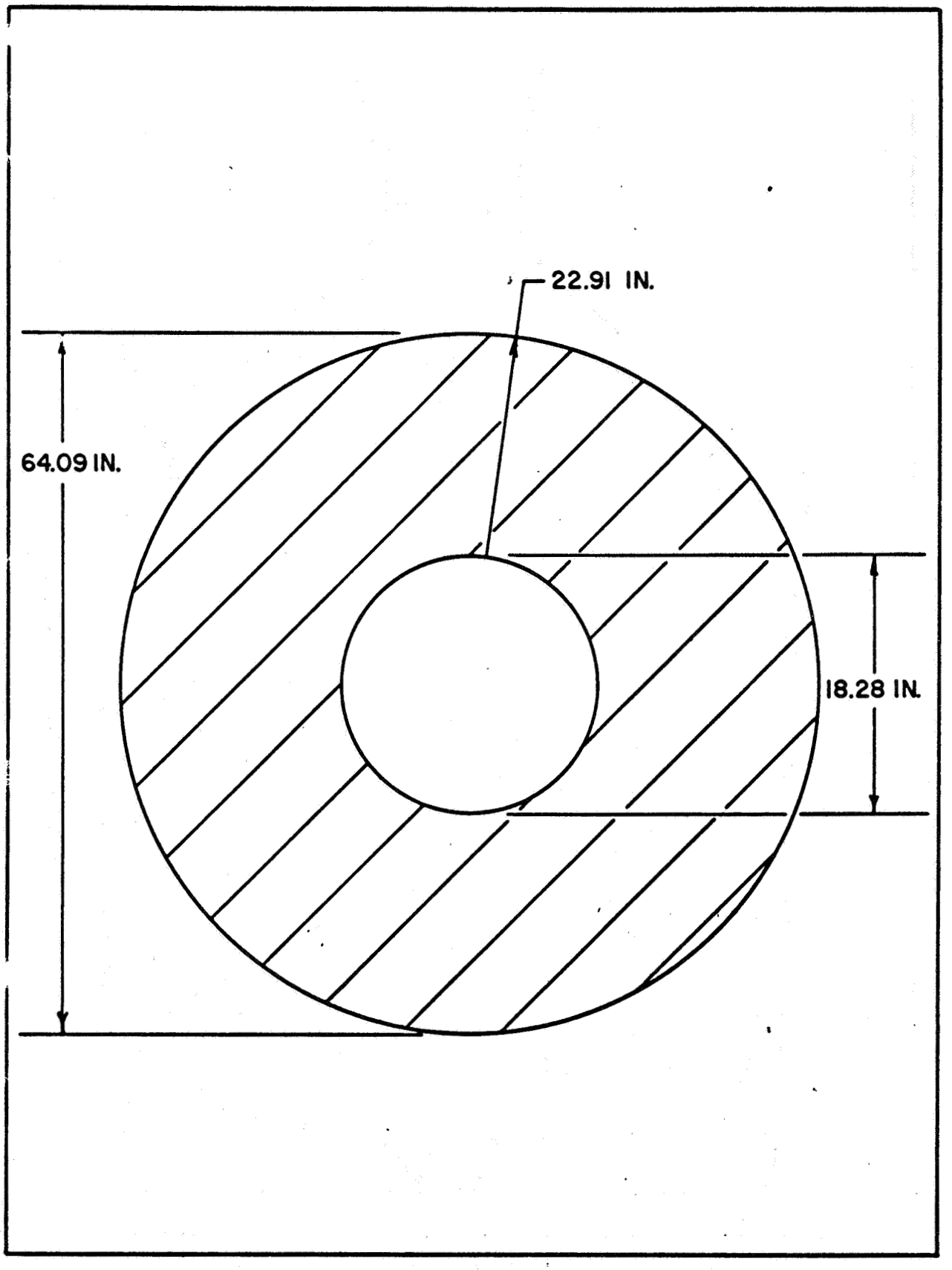

Figure 3 - Cross Section of Propellant Grain (65-SS-2 and -3)

TABLE I

MASTER DRAWING LIST

Drawing Number		Title
65-SS-2	65-SS-3	
IS36001	IS36001	Instrumentation Location, Subscale Nozzle
9U37525(01)	9U37525(02)	Rocket Motor, Final
9U37524	9U37524	Case and Closure Assembly, Loaded
9U37523	9U37523	Case and Closure Assembly
FU2905	FU2905	Case
9U34870	9U34870	Closure
IS30002	IS30002	Nozzle Assembly
IS30003	IS30004	Nozzle Assembly
U6797	U6797	Igniter Assembly
U3952	U3952	PYROGEN ASSEMBLY

IV. MOTOR COMPONENTS AND ANALYSES

A. NOZZLE

1. Design

Since the purpose of the 65-inch subscale nozzle was to evaluate the fabrication techniques and materials to be used in the 156- and 260-inch nozzle, the design concept for the subscale nozzle was the same as that used on the large nozzle. The nozzle design for the 65-inch motor can best be described as a 17.5-degree half-angle divergent, 45-degree half-angle convergent nozzle without provision for thrust vector control. The nozzles are made up of assemblies of heat- and erosion-resistant plastic materials reinforced with glass laminates and bonded into a steel housing. The same carbon, graphite, hi-silica, and glass tapes chosen for the 156- and 260-inch design because of their erosion resistance, performance, and low cost were used in the fabrication of the subscale nozzle. The ablative assemblies consisted of:

1. An entrance section of FM-5063 bias cut carbon tape at a 60-degree shingle angle

2. Three throat sections of bias cut FM-5064 graphite tape at shingle angles of 60, 45, and 30 degrees

3. An exit cone of MX-4926 carbon tape, MX-2600 silica tape, and MX-4600 glass tape, all warp cut and wrapped parallel to the centerline.

The housing was fabricated from a readily available, low cost AISI-4340 steel forging using state-of-the-art techniques.

The following is a summary of the major dimensions and weight of the nozzles:

Length (in.)	38.86
Attach flange O.D. (in.)	49.50
Exit cone I.D. (in.)	18.77
Initial throat dia. (in.)	7.49
Initial expansion ratio	6.28
Approximate weight (lbs)	780☆

☆Actual weights for two nozzles were different due to changes in the entrance insulation.

Figure 4 is an illustration of the 65-SS-2 nozzle showing the location and type of each material used in this nozzle. Figure 5 is a frong view of the same nozzle which shows the varying thickness of V-44 used in this design. Materials used in the assembly of this nozzle were as follows:

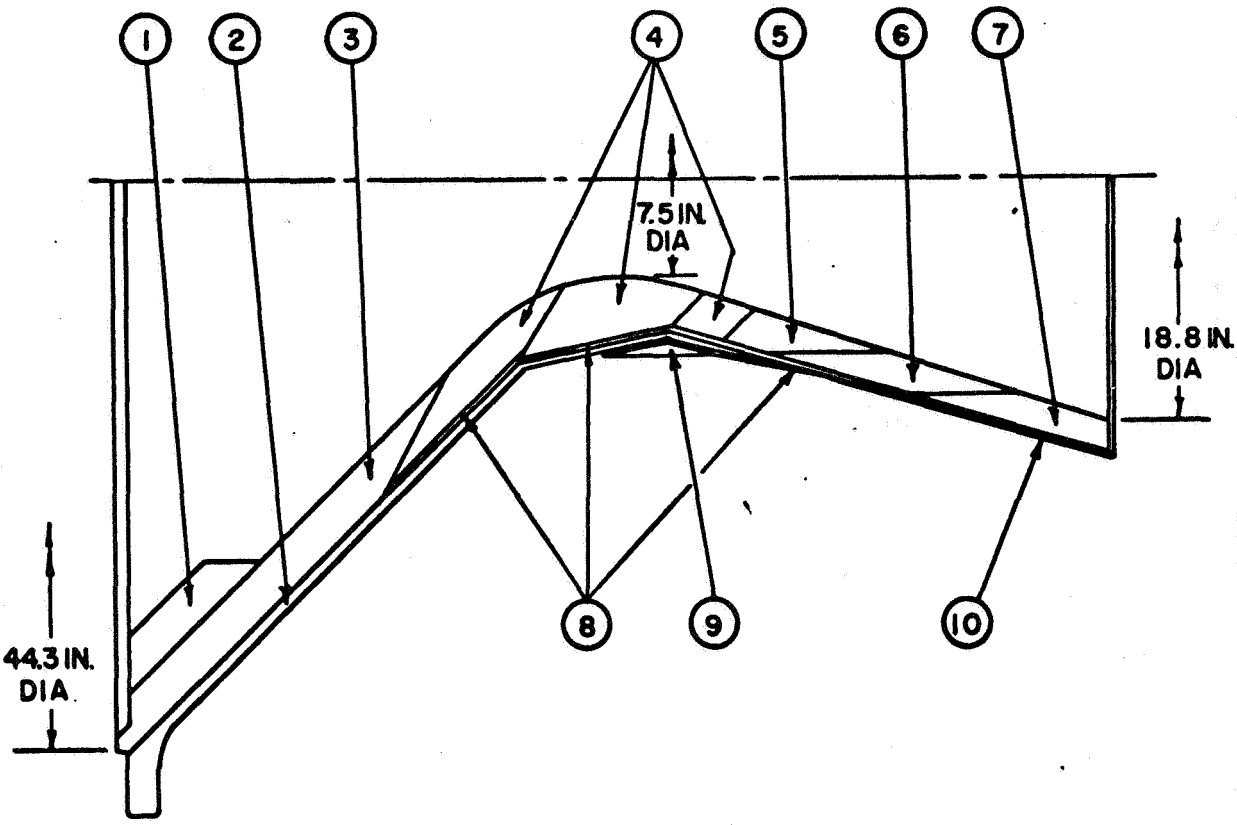

ITEM 1: GEN GARD V-44 INSULATION IN VARYING THICKNESS WITH V-61 JOINT FILLER

ITEM 2: AISI 4340 STEEL SHELL

ITEM 3: U.S. POLYMERIC FM 5063 BIAS CUT CARBON CLOTH, 60 DEG SHINGLE ANGLE

ITEM 4: U.S. POLYMERIC FM 5064 BIAS CUT GRAPHITE CLOTH, 60, 45, AND 30 DEG SHINGLE ANGLE

ITEM 5: FIBERITE MX 4926 WARP CUT CARBON CLOTH, PARALLEL TO CENTERLINE

ITEM 6: FIBERITE MX 2600 WARP CUT SILICA CLOTH, PARALLEL TO CENTERLINE

ITEM 7: FIBERITE MX 4600 WARP CUT GLASS CLOTH, PARALLEL TO CENTERLINE

ITEM 8: FIBERITE MX 4600 BI-DIRECTIONAL GLASS CLOTH-LAMINATES

ITEM 9: EPON 826 IMPREGNATED GLASS ROVINGS

ITEM 10: FIBERITE MX 4600 BI-DIRECTIONAL GLASS CLOTH, TIE LAMINATES

Figure 4 - Nozzle Assembly Materials, 65-SS-2 Motor

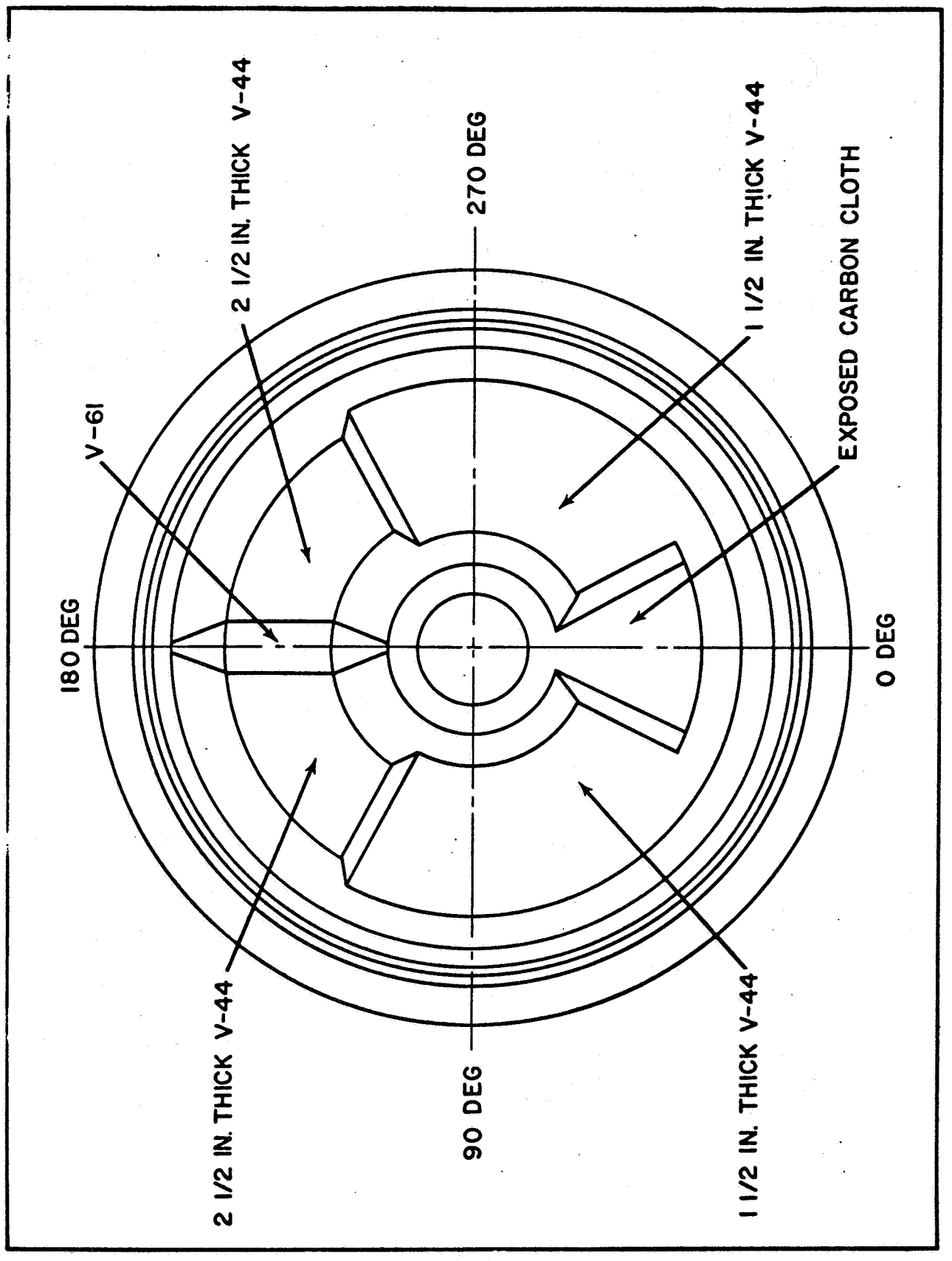

Figure 5 - Change in V-44 Thickness around Nozzle Entrance Section, 65-SS-2 Motor

1. Carbon filled phenolic resin was used in the forward throat-to-midthroat and the aft throat-to-exit cone ablative joints.

2. Epon 913 with Cab-O-Sil filler was used in the forward throat-to-entrance cone and midthroat-to-aft throat ablative joints. Joint filler was changed due to a problem with high temperature cure of phenolic which created a gap at the steel-to-ablative interface due to differences in the thermal coefficient of expansion.

3. Epon 826, temperature cured, was used to bond the midthroat and forward throat ablatives to the steel shell.

4. Epon 913, ambient cured, was used to bond the entrance cone and divergent cone to the steel shell and the V-44 to the carbon entrance insulation.

Figure 6 is an illustration of the 65-SS-3 nozzle showing type and location of each material used in fabrication of this nozzle. The materials used in the assembly were as follows:

1. Epon 913 with Cab-O-Sil filler was used in the forward throat-to-midthroat joint.

2. Carbon filled phenolic resin was used in the aft throat-to-exit cone ablative joint.

3. Zinc chromate putty was used in the midthroat-to-aft throat joint.

4. Epon 913 was used to bond all ablatives and the ORCO-9250 insulation to the steel housing.

The differences between the 65-SS-2 and 65-SS-3 nozzle designs were the results of problems which were encountered in the assembly of the 65-SS-2 nozzle and deficiencies found in the performance of the 65-SS-2 nozzle. The problems of differential thermal expansion which result from the use of an oven cured bond agent were present during the assembly of the subscale nozzle and were expected to be many times greater in the large nozzle. To avoid these problems, it was necessary to eliminate the oven-cured bonding adhesive, the oven-cured ablative joint filler, and the autoclave-cured tie laminates. Epon 913 adhesive, which had been used on previous Thiokol nozzles, was selected to replace the Epon 826 adhesive at the bond line. A series of materials was tested to select a replacement for the phenolic tie laminate; and from these, the Selectron Polyester resin with an ultraviolet catalyst was chosen. The detail results of the tests leading to this selection are covered in Section IV. D of Technical Note No. RPL-TDR-64-101.[1]

[1] SBR-35.764. 260-Inch Motor Demonstration and 156-Inch Motor Nozzle Test Program, Brunswick, Ga. Thiokol Chemical Corporation, Space Booster Division. 30 June 1964 (Confidential)

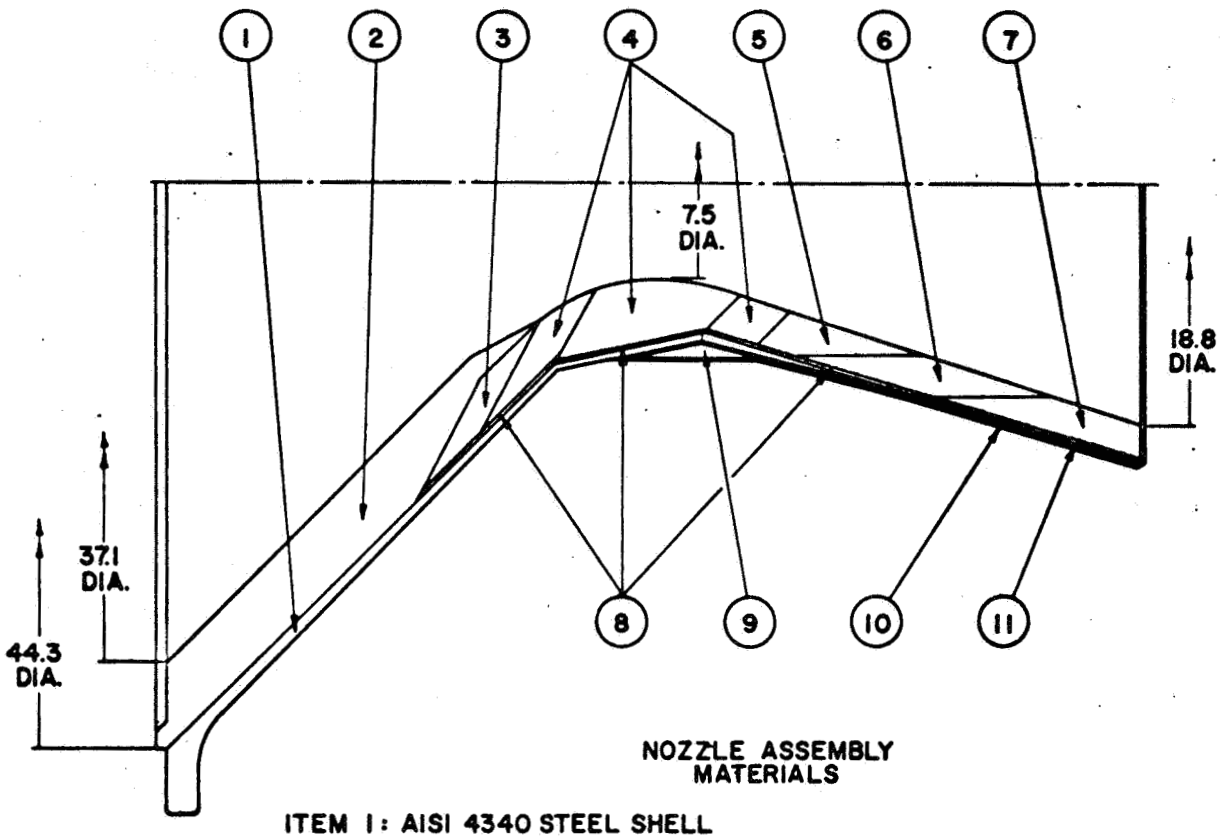

NOZZLE ASSEMBLY
MATERIALS

ITEM 1: AISI 4340 STEEL SHELL
ITEM 2: OHIO RUBBER ORCO 9250 ASBESTOS-SILICA FILLED BUNA-N FOR 180° OF CIRCUMFERENCE
TI-H7048 FOR 180° OF CIRCUMFERENCE
ITEM 3: U.S. POLYMERIC FM5063 BIAS CUT CARBON CLOTH, 60° SHINGLE ANGLE
ITEM 4: U.S. POLYMERIC FM5064 BIAS CUT GRAPHITE CLOTH, 60°, 45°, & 30° SHINGLE ANGLE RESPECTIVELY
ITEM 5: FIBERITE MX 4926 WARP CUT CARBON CLOTH, PARALLEL TO CENTERLINE
ITEM 6: FIBERITE MX2600 WARP CUT SILICA CLOTH, PARALLEL TO CENTERLINE
ITEM 7: FIBERITE MX4600 WARP CUT GLASS CLOTH, PARALLEL TO CENTERLINE
ITEM 8: PHENOLIC RESIN IMPREGNATED GLASS CLOTH
ITEM 9: EPOXY IMPREGNATED GLASS ROVINGS
ITEM 10: DYNA-THERM CORP. X-43-24
ITEM 11: POLYESTER RESIN IMPREGNATED GLASS CLOTH (SELECTRON 5003/5236)

Figure 6 - Nozzle Assembly Materials, 65-SS-3 Motor

The use of the Epon 913 as the adhesive for the ablative-to-shell bonding was started on the 65-SS-2 nozzle, and the tie laminate change was incorporated on the 65-SS-3 nozzle. Epon 913 with Cab-O-Sil filler was tried as a joint filler on some of the subscale joints but, due to unsatisfactory performance, it was replaced with zinc chromate putty. An effort was made to use the material selected for the 156- and 260-inch nozzle at the same area ratio locations in the subscale nozzle and with the same shingle angle; however, it did not always prove feasible. Table II shows a comparison of materials and area ratios for the 65-inch subscale and 260-inch nozzle designs. The size ratio of subscale to full scale nozzle did not make it economically sound to scale down the steel shell configuration.

Additional information concerning the 65-inch nozzle design detail can be found on Thiokol drawings 1S30002, 1S30003, and 1S30004, and in Thiokol specification SB-SP-118.

a. Thermal and Structural Analysis

The 65-inch subscale nozzle design was analyzed by the Wasatch Division of Thiokol. This analysis is presented in Report DLB-008-SA.[2] The nozzle thermal and structural analysis was divided into the following categories:

1. A heat transfer study, which included the effects of erosion, char, and temperature gradient on the plastic components

2. A stress analysis combining the effects of pressure and thermal environment on the steel shell and plastic ablative components

3. A discontinuity analysis of the steel shell

The heat transfer study gave a predicted erosion depth at six stations along the nozzle axis. The erosion depth was predicated on a design safety factor of two for the erosion rate. Erosion depth, char depth, and temperature profile were calculated for 1, 10, 40, 80, and 122 seconds at each station. The analysis predicted, subject to the safety factor of two for the erosion rate, that at a point 1.6 inches aft of the throat, the graphite material would be eroded away at the end of a 122-second firing. This was the least conservative point of the design. Since nominal web time for this motor was approximately 50 seconds, no design changes were made.

Using the temperature distribution calculated in the heat transfer analysis, a combined pressure and thermal analysis was made at the same six stations for burning times of 1, 40, 80, and 122 seconds on the basis of equating the conic elements to cylinders with equal curvature. This analysis determined the contact pressure necessary between thin concentric linearly elastic cylinders by equating the radial deflections of each due to the thermal and pressure loads. Each cylinder was considered thin enough so that an average temperature through its thickness could be used in calculating thermal loading. The stresses were calculated from the contact pressures

[2] Thermal and Structural Analyses, Subscale Nozzle Assembly, Report DLB-008-SA, Dwg. No. 1S30002, Brigham City, Utah, Thiokol Chemical Corporation, Wasatch Division 15 August 1965. (Confidential)

TABLE II

COMPARISON OF MATERIALS AND AREA RATIOS

Material and Wrap Angle	Location in Nozzle Area Ratio		
	65-SS-2 From/To	65-SS-3 From/To	156 & 260-Inch Design From/To
FM-5063 Carbon 60° to centerline	-16.0/-3.5	-4.7/-2.1	-4.8/-1.4
FM-5064 Graphite 60° to centerline	-3.5/-1.2	-2.1/-1.2	-1.4/-1.08
FM-5064 Graphite 45° to centerline	-1.2/1.4	-1.2/1.4	-1.08/1.01
FM-5064 Graphite 30° to centerline	1.4/1.8	1.4/1.8	1.01/1.12
MX-4926 Carbon parallel to centerline	1.8/3.0	1.8/3.0	1.12/3.2
MX-2600 Silica parallel to centerline	3.0/5.0	3.0/5.0	3.2/exit
MX-4600 Glass parallel to centerline	5.0/exit	5.0/exit	See Note 2

NOTES: 1. Minus sign indicates convergent section of nozzle

2. The glass was eliminated from the full scale nozzle on the basis of 65-SS-2 static test data

determined. At the stations considered, the tensile stresses were found to be low. The minimum margin of safety reported for tension in the nozzle ablatives was 2.77. High compressive stresses in the entrance cone and exit cone were found but margins of safety are not presented since these stresses were not considered critical to the performance of the nozzle.

The discontinuity analysis considered the nozzle attachment joint and the two slope discontinuities in the steel shell. At the nozzle attachment joint, the lowest margin of safety of 0.41 was determined for the bolts due to combined shear and tensile stresses. The discontinuity in the entrance section of the nozzle shell had a minimum margin of safety of 0.40 with respect to the hoop stress at this point. The discontinuity in the exit cone section had a minimum margin of safety of 2.96 with respect to the hoop stress at this point. The discontinuity analysis used a MEOP of 840 psi for the pressure load in this area, which means that these are conservative margins of safety.

The analysis concluded that the design of the nozzle was adequate from both a structural and a thermal standpoint.

2. Fabrication

a. Ablatives

Processing of ablative components for the subscale nozzle was planned to simulate, as nearly as possible, that planned for the 156-2C-1 and 260-SL-1 nozzle components. Since tape wrapping was the basic process selected for forming ablative materials into the desired shapes prior to curing, this was the desired fabrication approach for subscale components. Problems were encountered, however, which were direct results of the combination of relatively small diameter and large thicknesses of the subscale nozzles. These problems prevented tape wrapping of all ablatives by the conventional approach planned for full-scale parts.

(1) Bias Tape Wrapping

One of the major difficulties experienced was in forming wide bias tape around the small-radius subscale mandrels at the required wrapping angles. During the winding process, there is a tendency for the inner edge of the tape to contract, increasing the fiber density (yarns per inch) in this area. At the same time, the outer tape edge must elongate. The minimum radius about which a given tape width can be successfully wrapped, is therefore, dependent upon the maximum achievable difference between inner edge and outer edge distortion. When a tape has been distorted to its natural limit during an angle-to-centerline wrapping process, additional attempts to increase the elongation of the outer edge and the contraction of the inner edge will result in buckling at the inner edge, causing ripples or folds to appear in the tape. These ripples will become permanently wound into the part if allowed to pass under a compacting roller. This relationship can be mathematically shown as follows:

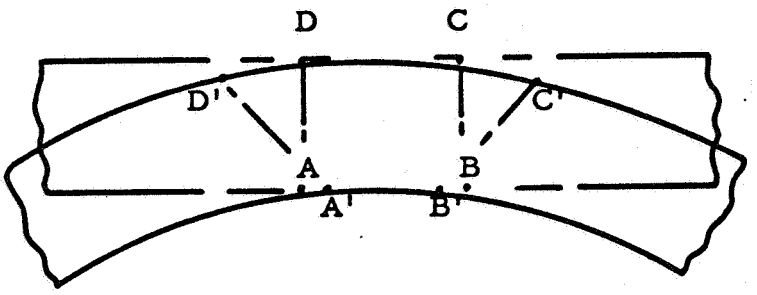

H = ratio of edge length after wrapping

$$H = \frac{C'D'}{A'B'}$$

Or

$$H = \frac{\frac{C'D'}{CD}}{\frac{A'B'}{AB}}$$

The following takes place in one revolution:

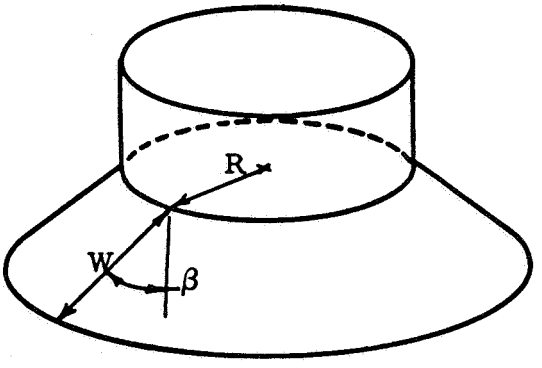

	L"	= length around inner edge/one revolution
	L'	= length around outer edge/one revolution
	W	= as-wrapped width
	H	= max. ratio of outer edge to inner edge tape distortion
	L"	= $2\pi R$
	L'	= $2\pi (R + W \sin \beta)$
but	L'	= HL" for maximum lengthening
	HL"	= $2\pi (R + W \sin \beta)$
therefore		
	H $2\pi R$	= $2\pi (R + W \sin \beta)$
	HR	= $R + W \sin \beta$
	HR-R	= $W \sin \beta$
	H	= $\frac{W \sin \beta + 1}{R}$

It was determined experimentally that H values up to 1.30 could be successfully wrapped. Fabric weave and basic material handling characteristics are, of course, major contributors to the value of H.

Evaluation of the geometry of the bias tape components showed that the small end of the 65" entrance cone ablative component could not be wrapped by the techniques selected for the 156- and 260-inch nozzle. Approximately 2 inches of the larger end of the entrance cone could be wrapped due to its large diameter, and the aft throat could be wrapped due to the 30-degree shingle angle selected for this component. Table III indicates which ablative components were wrapped and those which were fabricated by the hand layup technique.

Since one of the most important objectives of the subscale program was to verify performance capability of the selected ablative materials, a fabrication process was required which would provide the same degree of ablative performance attainable with tape wrapping. The wrinkles or folds in the plies of ablative material resulting from tape wrapping full-width tape were objectionable because they significantly lowered the integrity of the part from a physical properties standpoint, represented a potential increase in erosion rate resulting from resin-rich pockets in the fold-over areas, and disturbed fiber orientation.

The following approaches were evaluated as means to eliminate wrinkles and folds in the subscale parts while maintaining ply orientation and performance potential:

1. Use a new material in which the weave of the fabric reinforcement permits greater distortion about a radius without buckling.

2. Use available, full-width tape, but slit the outside edge of the tape during the winding process to reduce the width of material that must be deformed without wrinkles.

3. Wrap three different widths of tape, alternating the position of these widths to obtain overlaps between adjacent layers. Each width of tape would be capable of being wound around the component without inducing wrinkles.

4. Distort the weave of the standard tape material. If a 45-degree bias tape is mechanically distorted to increase the width of the tape, then the angle of the fibers in that tape will be changed from 45 degrees to some angle greater than 45 degrees. This will provide greater distortion capabilities for the tape materials since the fibers must first return to the initial weave position before further distortion can be accomplished.

5. Use a hand layup process. Arc-shaped patterned pieces are cut from broad goods and applied by

TABLE III

ABLATIVE COMPONENT FABRICATION TECHNIQUES
(65-SS-2 AND -3)

Component	Wrapping Angle, degree	65-SS-2 Motor Nozzle	65-SS-3 Motor Nozzle
Entrance Cone	60	Hand Layup (See Note 1)	See Note 2
Forward Throat	60	Hand Layup	Hand Layup
Midthroat	45	Hand Layup	Hand Layup
Aft Throat	30	Wrapped	Wrapped
Exit Cone	Parallel to Centerline	Wrapped	Wrapped

NOTES: 1. The first 2 inches of material on the extreme forward end of this component was wrapped; remainder of component was hand laid up.

2. The nozzle design for this motor did not contain an ablative tape entrance cone.

operators around the mandrel. Since the pattern of the pieces provides the required distortion capability, full-width tape can be applied at the selected shingle angle.

Hand layup of arc-cut patterns was selected as the processing technique providing the best control of ply orientation, highest degree of structural integrity, and best ablation resistance. The layup pattern which was used is described as follows:

1. Arc segments are cut from broad goods with each arc section having a minimum length of 6 inches.

2. Layup is performed so that each arc segment overlaps one-half to two-thirds of the preceding arc segment. Layup continues in the direction initiated until the required thickness of material is achieved.

3. Each arc pattern is tacked to the preceding piece by use of heat from an electrical air blowing heat gun. The heat also softens the material for the action of the debulking roller.

4. Debulking is accomplished by passing each arc-cut pattern under a pressure roller while it is still soft. The debulking roller is a part of the winding equipment.

5. Cooling of the debulked segments is performed using expanding compressed air. This cooling assists in maintaining the compression impacted to the material by the debulking roller.

6. Mandrels are remachined in the areas of the hand layup of tape arc patterns to allow for subsequent removal of material from the ID of each component. Approximately 1/8 inch of material is removed from the inside of each cured ablative component, thereby permitting removal of uncontrolled edges of the arc-cut patterns of tape next to the mandrel surfaces.

The process described above was used in fabrication of the bias tape components, as indicated in Table III. The results discussed in Section IV. A. 3 of this report indicate that the performance was equal to or better than predicted, which proves the process to be acceptable for ablative fabrication.

(2) Warp Tape Wrapping

The use of warp tape and parallel-to-centerline wrapping for the exit cone fabrication also led to problems which were not necessarily peculiar to the subscale nozzle but were compounded due to the large wall thickness (T)

and small radius (r) of the component. The r/T ratio for the subscale nozzle was approximately 3, as compared with 10 for the 156- and 260-inch nozzle exit cone. The significance of the r/T ratio can best be explained by an examination of the mechanics of the wrapping and cure process for a warp cut tape.

Each raw material has a characteristic ply thickness (t) which is reduced during the winding process to a new thickness (t_2). During cure, further thickness reduction occurs, yielding a cured ply thickness (t_3). With each ply of tape reducing in thickness during cure by the value $t_2 - t_3 = \Delta t$, the radius of the tape-wound component will change by an additional value, $N \times \Delta t$, wherein N represents the total number of plies applied.

R_i = as-wrapped outside radius

R_c = cured outside radius

$R_i - R_c = N\Delta t$

This reduction in radius represents a corresponding reduction in circumference.

$$\Delta \text{ circumference} = 2\pi \Delta t N$$

$$\text{compressive strain } \epsilon = \frac{N\Delta t}{R_i} \text{ in./in.}$$

The total reduction in circumference of the tape-wound components must be accommodated by linear compression of the uncured tape material, which will wrinkle if allowable compressive characteristics are exceeded by a sizable change in circumference.

Experimental results obtained during the fabrication of subscale components indicated that compressive limits vary from one material to another. The limit varied from approximately 0.006 in./in. for MX-4926 carbon material to 0.010 in./in. for MX-2600 silica material.

A high percentage of debulk during the wrapping process means a small Δt and consequently low compressive strain and less chance for wrinkling. The larger the ratio of radius to thickness, the larger the circumference available to absorb the change in circumference which also results in a lower compressive strain. Both of these improvements existed in the large 156- and 260-inch exit cone which provided a high degree of confidence that these parts could be fabricated without a severe wrinkling problem.

Three attempts were made to wrap a wrinkle free exit cone for the subscale nozzle without success. With equipment limitations and the small size discussed above, a sufficient percentage of debulk could not be attained to prevent wrinkles. Figure 7 shows one of the subscale exit cones which had been subjected to a hydroclave cure. In normal hydroclaving operations, buckles or wrinkles will form on the outside of the components when deformation becomes too great. Wrinkles will normally dampen out toward

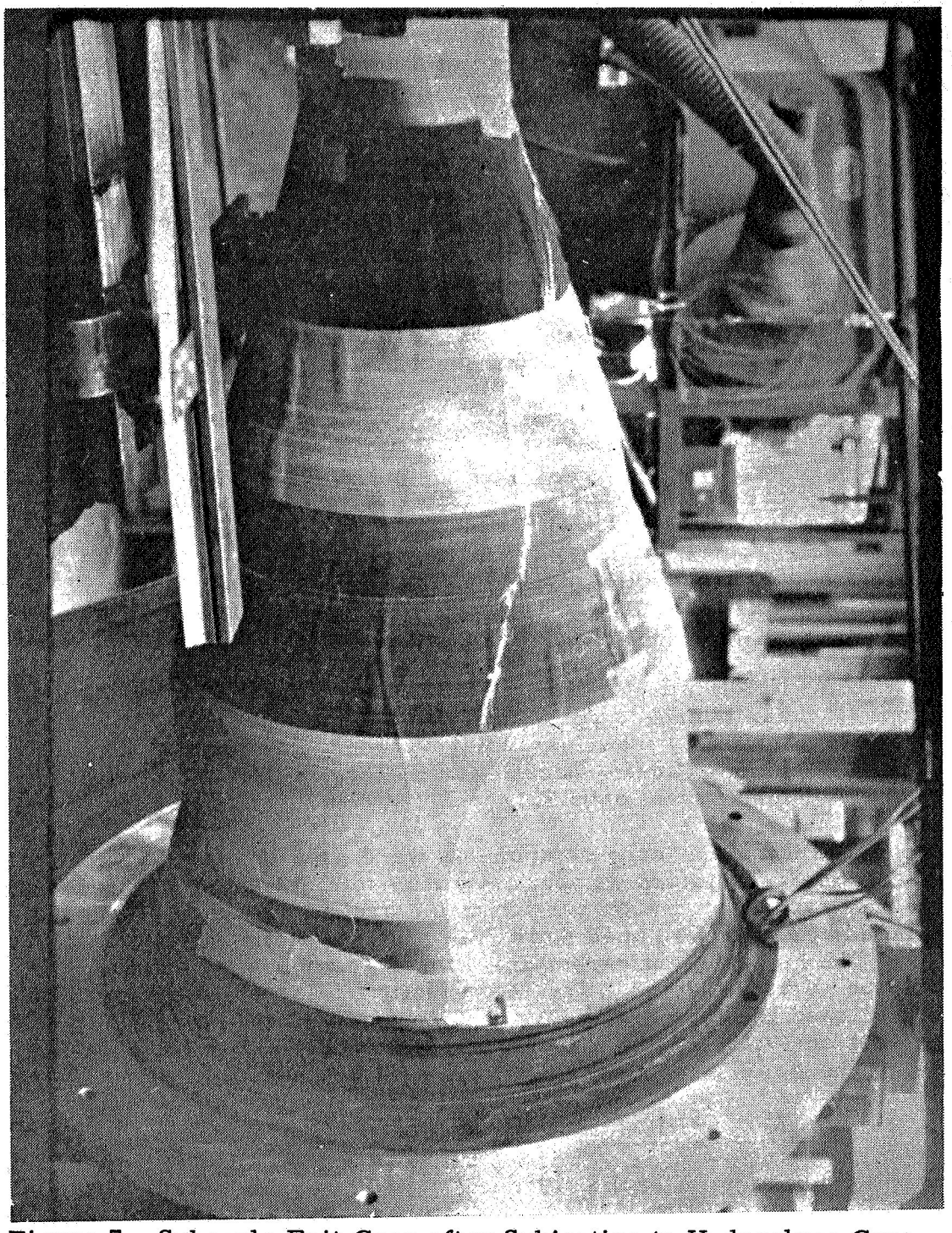

Figure 7 - Subscale Exit Cone after Subjection to Hydroclave Cure

the inside surface of the component. These wrinkles can, therefore, be described as outside-to-inside wrinkles, and were found on the first two 65-SS exit cones. The wrinkles in both instances progressed almost to the inside surface of the component instead of damping out within 50 percent of the wall thickness, as would normally be the case with a component wound with a moderate degree of debulking.

The third exit cone was characterized by inside-to-outside wrinkles in the MX-4926 carbon material. These wrinkles were formed by buckling of layers of tape originating from the inside surface and damping out as the plies progressed toward the outside surface. The following three conditions may have caused the inside-to-outside wrinkling condition:

1. Improper guiding and orienting of tape edges with respect to the mandrel so that edges of several plies of tape were away from the mandrel surface. Wrapping over a pocket or gap created in this manner would leave subsequent plies wrapped over this area unsupported. Wrinkling could then occur when material was forced into these pockets by pressure curing.

2. Tension in the tape. Previous work substantiates the possibilities of winding in wrinkles if the initial layers are not properly debulked.

3. Nylon tape, applied to the outside surface of the component to reduce or eliminate outside-to-inside wrinkles, may have produced compressive forces causing buckling of materials because of insufficient debulking.

The second and third exit cone components were used in the nozzle for the 65-SS-2 and 65-SS-3 motors without any noticeable detriment from the wrinkled ablative. The carbon section of the second exit cone component was replaced before it was used due to the sharpness and amplitude of the wrinkles. The replacement carbon insert was water soaked on two occasions due to bag failures. The large factors of safety for this component allowed the component to be used in spite of the moisture. Test results (Section IV.A.3 of this report) show a comparison of the performance of the two exit cones.

(3) Ablative Processing

Following the wrapping of each component, it was subjected to a hydroclave cure at 1000 psi for the times and temperatures listed in Table IV. The table indicates that several changes were made in the times and temperature used in the ablative cure cycle and in the post-cure requirements. Changes were made in an effort to achieve a debulking phase at reduced pressure in order to minimize the wrinkling tendency in the portion of the cycle where the phenolic has not jelled. The ablatives for the second subscale nozzle were post-cured for 48 hours in an oven atmosphere in an effort to provide better dimensional stability. The problems encountered in bonding the forward throat ablative into the nozzle shell for the 65-SS-2 motor emphasized

TABLE IV

CURE AND POST-CURE CYCLES OF SUBSCALE NOZZLE ABLATIVE COMPONENTS

Nozzle for Motor	Component	Material	Cure	Post-Cure	Acetone Extractables (Percent)		
					I. D.	Center	O. D.
65-SS-2	Entr. Cone	Carbon FM-5063	7 hrs at 350 F	None	2.30	2.50	2.94
65-SS-2	Fwd. Throat	Graphite FM-5064	7 hrs at 350 F	None	5.42	--	3.75
65-SS-2	Midthroat	Graphite FM-5064	7 hrs at 350 F	None	5.28	--	4.73
65-SS-2	Aft Throat	Graphite FM-5064	7 hrs at 350 F	None	4.12	--	3.79
65-SS-2	Exit Cone	Carbon MX-4926	7 hrs at 300 F	None	0.48	0.37	0.49
		Silica MX-2600			--	--	0.40
		Glass MX-4600			0.40	--	0.39
65-SS-3	Fwd. Throat (Note 2)	Carbon FM-5063 Graphite FM-5064	4 hrs at 350 F	48 hrs at 300 F	3.50	3.96	3.03
65-SS-3	Midthroat	Graphite FM-5064	4 hrs at 350 F	48 hrs at 300 F	2.96	3.94	--
65-SS-3	Aft Throat	Graphite FM-5064	4 hrs at 350 F	48 hrs at 300 F	5.92	5.58	4.23
65-SS-3	Exit Cone (Note 3)	Carbon MX-4926	4 hrs at 300 F	48 hrs at 300 F	0.65	0.56	0.32
		Silica MX-2600			--	0.38	0.70
		Glass MX-4600			0.83	0.53	--

NOTES: 1. Acetone extraction tests were for information only and test samples were not available at all locations.

2. The forward throat for this unit was a carbon and graphite composite.

3. The carbon portion was subjected to two partial cure cycles due to a hydrobag leak.

the probability of a lack of dimensional stability in phenolic laminates. This problem and the solution which led to the addition of the post-cure cycle are discussed in detail in the next section of this report.

Following the cure and post-cure cycles, ablative sections were machined on the O.D. to the configuration required and a bidirectional glass laminate applied. Figure 8 shows the glass being applied to the entrance cone for the 65-SS-2 nozzle. Difficulties were experienced in obtaining a wrinkle-free glass laminate. Studies concerning the laminate layup techniques will also be discussed in the next section. The ablative and glass were then subjected to radiographic inspection both tangential and parallel to the ply in an effort to detect any unbond between the glass and ablative, or delaminations within the ablatives. Following inspection, individual ablative assemblies were ready for assembly into the shell.

(4) Elastomeric Insulation Fabrication

The first nozzle unit for motor 65-SS-2 had a section of V-44 insulation in the convergent section. This V-44 insulation covered the majority of the carbon phenolic as shown in Figure 5. The insulation was fabricated by laying up pattern pieces of the V-44 in a female mold. The edges of each piece were cut at an angle to the ply surface with a hot knife and vulcanized to the preceding ply with the knife. The ply was then stitched to the preceding layer with a roller, ensuring the removal of entrapped air. The layup was then subjected to an autoclave vulcanize cycle and match machined to mate with the carbon section of the convergent ablatives.

The convergent insulation for the 65-SS-3 nozzle was composed of a 180-degree arc segment of an asbestos and silica-filled Buna-N rubber fabricated by the technique described above for the first nozzle unit. The other 180-degree segment consisted of Thiokol insulation TI-H704B troweled in place at the Wasatch Division of Thiokol Chemical Corporation.

b. Steel Shell

The steel housings for the 65-inch subscale nozzles were fabricated by circumferentially welding a series of alloy steel, Type AISI-4340, forgings. Two units of the configuration described on Thiokol drawing 1S30002B were made for these nozzles. After all welding had been completed and the welds inspected, the housings were normalized and tempered in accordance with Specification MIL-H-6875 to a yield strength of not less than 150,000 psi at 0.2 percent offset. Welding was in accordance with Specification MIL-W-8611, and the soundness of the welds conformed to Specification MIL-R-11468, Standard II. Figure 9 shows one of the completed shells during the final inspection operation.

c. Nozzle Assembly

The planned assembly sequence for the subscale nozzle was modified several times to accommodate availability of components and to avoid repetitive type problems. The planned sequence was to install one ablative component at a time, starting with the exit cone and working forward. Each piece would be dry fitted to the steel shell, removed and machined, as required, bonded to the steel shell, and machined on the face which was

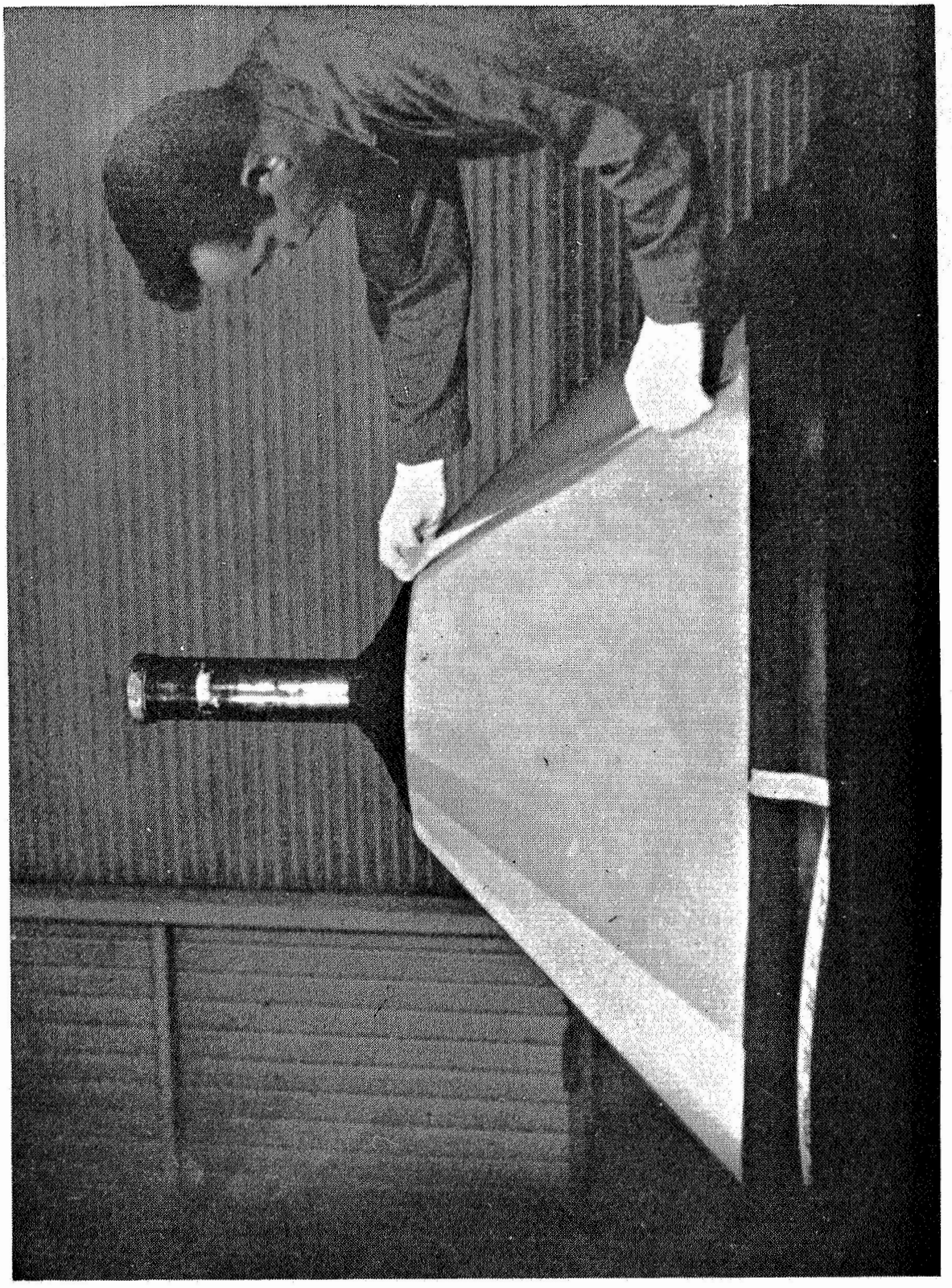

Figure 8 - Application of Bidirectional Glass Laminate to 65-SS-2 Nozzle Entrance Cone

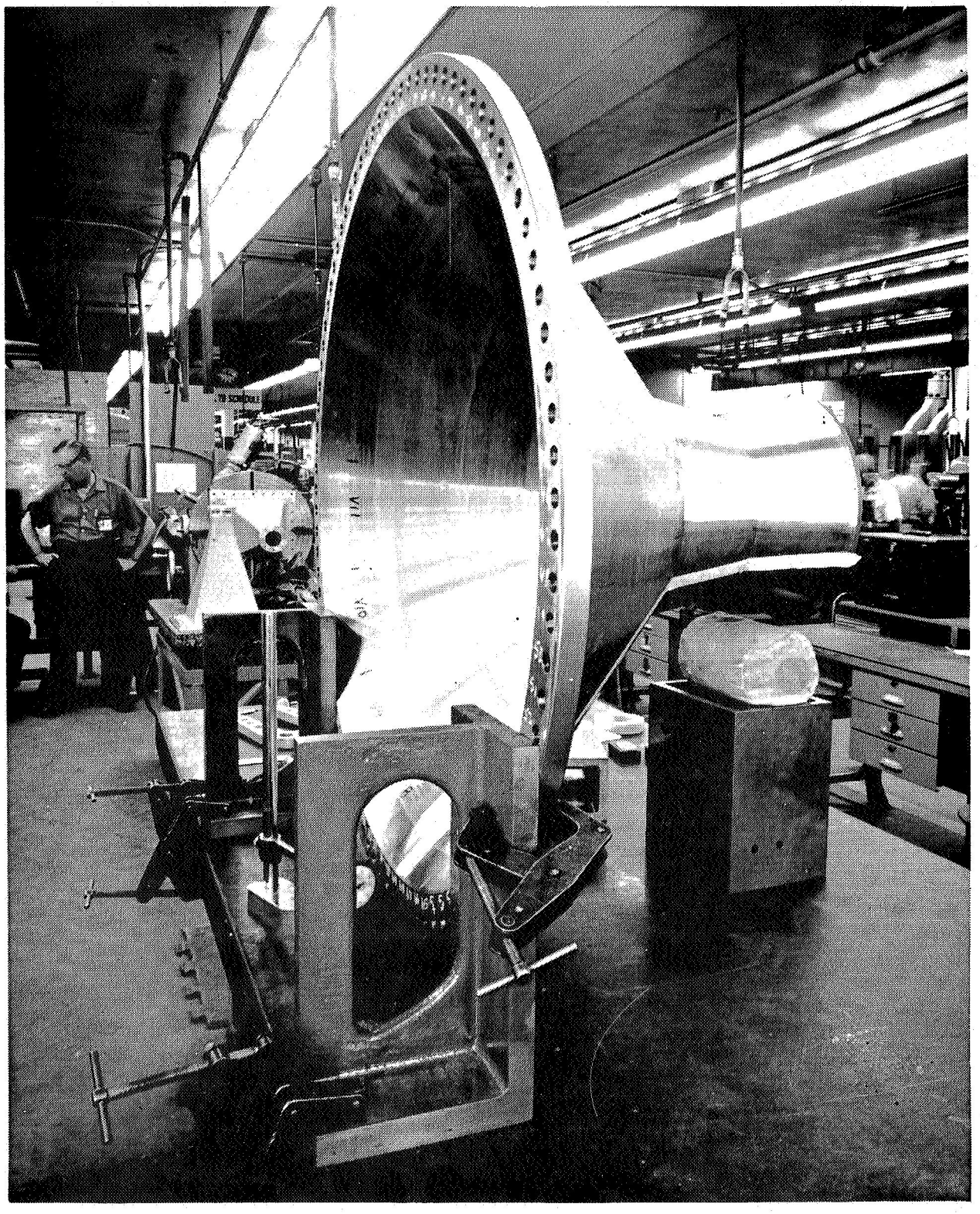

Figure 9 - Subscale Nozzle Steel Shell During Final Inspection

to mate with the next ablative component. The actual sequence for the nozzle for motor 65-SS-2 was as follows:

1. The midthroat ablative was dry fitted to the shell, bonded to the machined steel shell with Epon 826 adhesive, temperature cured at 185 F, and machined on the forward face to mate with the forward throat.

2. The forward throat was match machined on the outside and aft end to mate with the midthroat and subsequently bonded to the steel shell with Epon 826 adhesive and cured at 185 F. The joint between the midthroat and forward throat was filled with carbon filled phenolic resin. When the machining was started on the forward end of this ablative, an unbond condition was visually located around the entire circumference of the part. This condition was repaired with a very low viscosity Epon 815 adhesive system.

3. The entrance cone was machined on the aft end and outside to match the forward throat. This component was bonded to the steel shell with Epon 913 adhesive and ambient cured. The joint between the entrance cone and forward throat was filled with Epon 913 adhesive with a Cab-O-Sil filler.

4. The aft throat ablative and the exit cone ablative were bonded together with a carbon filled phenolic resin. The structural laminate was then applied over the assembly and machined to fit the steel housing and aft end of the midthroat.

5. The interior and exterior surfaces of the divergent section of the steel shell to which the tie laminates would be bonded were grit blasted. The joint between the midthroat and divergent cone assembly was filled with Epon 913 with Cab-O-Sil filler. The divergent cone assembly was bonded to the shell with Epon 913 and ambient cured.

6. Phenolic impregnated bidirectional glass tie laminates were applied on the outside of this assembly and the entire unit subjected to a 300 F and 200 psi autoclave cure. The entire unit was bagged for this cure to ensure that the pressure would assist in maintaining the ablative in place.

7. Wet-dip, ambient curing epoxy rovings were applied on the outside of the assembly in the throat area and cured at room temperature.

8. The V-44 entrance insulation was mated with the

entrance cone carbon material and bonded in place with Epon 913 ambient cure adhesive. The V-groove in the V-44 was filled with General Tire V-61 material.

9. The unit was painted and shipped to Thiokol's Wasatch Division for testing.

Bond lines between the steel housing and ablatives on the nozzle assembly were 100 percent ultrasonic inspected. Bond lines between the tie laminate and the divergent cone and steel housing were spot checked by tangential X-ray. Ablative-to-ablative joints were also spot checked by tangential X-ray.

Assembly of the nozzle for the 65-SS-3 motor varied from the 65-SS-2 nozzle assembly procedure due to material changes and component availability. The 65-SS-3 nozzle was assembled as follows:

1. The midthroat ablative was fitted to the shell and machined as described under the 65-SS-2 nozzle assembly sequence. However, Epon 913 adhesive was used as the bonding agent for the second unit.

2. The forward throat ablative was match machined to the midthroat and bonded to the steel shell with Epon 913. The ablative-to-ablative joint was filled with Epon 913.

3. The divergent cone assembly was completed as described under the 65-SS-2 nozzle assembly sequence. Radiographic inspection revealed what appeared to be cracks or delaminations in the outer surface of the aft throat. The aft throat was subsequently removed from the subassembly and replaced with a new ablative section. The divergent cone assembly was then bonded in place with Epon 913. The joint between the midthroat and divergent cone assembly was filled with zinc chromate putty.

4. Due to assembly problems associated with temperature cycling of a full scale nozzle, the tie laminate material was changed from phenolic impregnated bidirectional glass cloth to a wet layup, ambient cure system of polyester resin with an ultraviolet catalyst. The tie laminate layup was completed and cured.

5. Ambient cure rovings were applied in the throat area over the tie laminates.

6. A 180-degree segment of Ohio Rubber ORCO-9250 was bonded directly to the steel housing in the entrance section using Epon 913 adhesive.

7. Thiokol TI-H704B insulation was hand-troweled into the remaining 180 degrees of the entrance section and cured in place at 135 F.

8. Dyna-Therm Corporation's X43-24 material was applied over the polyester resin and tie laminate to provide insulation for the low temperature resin.

Operations 7 and 8 were conducted at the Wasatch Division of Thiokol Chemical Corporation. The bond lines between the ablative materials and the steel housing were ultrasonically inspected. The elastomeric insulation materials were radiographically inspected.

d. Ablative Fabrication Problems

During fabrication of the ablative components for the 65-inch subscale nozzles, numerous problems were encountered in materials and processes that required change and modification to planned fabrication techniques. A portion of these problems resulted in changes to fabrication parameters for the large nozzle ablative components, while some problems were unique to fabrication of subscale components. The following are problems encountered and resultant solutions.

(1) Tape Heating

Heating of tape materials as they are applied to the mandrel surface is necessary to achieve proper tacking and laydown. This heating must be performed within defined ranges of temperature to assure that material is heating to a sufficient point to achieve desired tacking and neckdown, but not to such an advanced point that resin cure or significant reduction of flow occurs. Subscale components were fabricated using heat guns for the source of heat. Heat guns are devices that produce heat electrically and distribute that heat by means of an air blower. Considerable variations were encountered in actual tape temperature during some of the subscale winding and layup processes. Quartz lamps were ultimately selected for the full scale nozzle as providing the best temperature control for components which are to be mechanically wrapped.

(2) Tape Cooling

When heat is applied to the tape materials during the winding process to achieve tacking, it is frequently necessary to cool the tape after it has passed under the debulking roller to prevent springback of the material. The temperature of the debulking roller must be controlled also, as a high temperature will cause the roller to pick up resin from the tape. The method of cooling used on some of the first subscale components was to pass pressurized line air through a drum of dry ice, thereby chilling the air. The chilling, however, reduced the temperature of the line air below the dew point. This temperature drop caused moisture particles to be condensed and blown through the line and, in most cases, onto the part being wrapped. The amount of moisture being added to the tape material during the winding process varied, depending on the relative humidity of the wrapping area. The addition of condensation was an undesirable situation because water is a by-product of the phenolic resin cure mechanism. Adding water to the uncured material has

the same effect as adding volatiles to the material. As free phenol tends to be water-soluble, the effect on the material is to increase resin flow and to increase volatile content, thereby approximating a material that is greener than it was initially. Consideration was given to modification of the cure cycle to permit drying or removal of a great portion of the wound-in water before actual cure of the part. However, total assurance that the water had been removed satisfactorily could not be attained, and there was a danger that water would be cured into the component in the form of volatiles that would be released destructively during the motor firing. Expanding of compressed air was finally perfected as the cooling medium in the wrapping process.

(3) Tape Debulking

Debulking of the tape materials during the winding process to achieve the highest as-wrapped density possible is desired in order to minimize tape movement and subsequent wrinkling that could occur during high pressure hydroclave curing. The debulking factor is defined as the ratio obtained by dividing the difference in the thickness of as-purchased material and as-wrapped material by the difference in thickness of as-purchased material and as-cured material. If a relatively low debulking factor is achieved in the winding process, high pressure hydroclave curing will cause movement of the tape, resulting in wrinkling and a change of the shingle angle. In-process control of the debulking factor is necessary to eliminate several variables that could be introduced during the curing cycle where tape movement is unseen and undetected until the part is finally cured. Initial attempts to fabricate subscale components were based upon debulking factors in the range of 55 percent. However, the problems associated in achieving good quality components were such that it was quickly realized that a higher debulking factor was required. A debulking factor of 80 percent minimum, and preferably 90 percent or greater, was established as the goal during subscale fabrication. In-process parameters for all full-scale components, therefore, reflected the requirements for achieving a higher debulking factor, i.e., one above 80 percent minimum.

(4) Tape Tensioning

Successful tensioning of bias tape is not as easily achieved as is the case with tensioning warp-cut tape. Bias tape tends to reduce its width as the fibers are stretched, and to change the angle of orientation with respect to the edge of the fabric. Because of the lack of continuity of the fibers with bias tape, it is not possible to use as high a tension per inch of width as for warp-cut tape. As a result, virtually no tension can be applied to bias tape during the winding process; only a guiding of the material can be accomplished reliably. With judicious use of heat and debulking pressure, applying the tape without tension does not constitute a major problem. However, guiding the tape onto the mandrel, as on the subscale aft throat ablative, requires the orientation of the inner edge of each tape layer to the mandrel surface. Ideally, the inner edge of each layer of tape would be in contact with the mandrel, and would neither form a gap between the edge of the tape and the mandrel nor overlap and ride up onto the mandrel. If the edge of the tape with respect to the mandrel is relatively uncontrolled, then resin-rich pockets will be formed on the inner surface of the component. The resultant orientation of the fibers will be relatively random. Hand-guidance and trim

of the overguided edges was used on the subscale nozzle aft throats in order to prevent a schedule delay. A practical solution is still not available for this operation.

(5) Ablative Dimensional Stability

A separation was found between the steel shell and the forward throat insert during the process of facing the forward end of the forward throat insert. The separation extended 360 degrees around the component at gap widths varying from 1 to 6 mils and affected approximately 40 percent of the total bonding area. This separation emphasized the problem of a lack of ablative dimensional stability and the probability of a varying coefficient of thermal expansion depending on the state of cure for each type of material. In an effort to better define the actual coefficient of thermal expansion versus state-of-cure and the magnitude of the shrinkages taking place in the ablatives, a series of tests was conducted at Rohr Corporation. Since shorter times in the hydroclave or oven and lower temperature were both desirable from an economy standpoint, these were investigated to ascertain the effectiveness of each. Production hydroclave curing and 265 F post-cure temperatures were evaluated using a specimen taken from the graphite midthroat segment of the subscale nozzle for the 65-SS-3 motor. Post-curing consisted of a 48-hour production cycle plus an additional 48-hour laboratory cycle to obtain a total post-cure of 96 hours at 265 F. A second laboratory 300 F post-cure cycle was investigated by employing flat press cured Fiberite MX-4926 carbon laminate post-cured for 24, 48, and 96 hours. Resulting data are tabulated in Table V.

These data indicate that a 265 F post-cure cycle of 48 hours is effective in stabilizing thermal characteristics, particularly with respect to the coefficient of thermal expansion. Elevated temperature shrinkage and net shrinkage were improved with this post-cure schedule.

The 300 F post-cure of the laboratory-cured Fiberite MX-4926 carbon laminate indicated attainment of acceptable stability with a 24-hour cycle. This material, however, exhibited excellent stability without post-curing. In addition, post-curing unexpectedly resulted in an increase in the coefficient of thermal expansion rather than the normal decrease. A second test on the as-cured specimen resulted in a coefficient of 4.7×10^{-6}, which verified the initial data. Complete details of the test plus additional data on specimens of silica and glass materials are contained in Report R-1026.[3]

(6) Glass Laminate Wrinkling

Occurrence of longitudinal wrinkles in the cured bidirectional glass laminate of the 65-SS-2 divergent cone created the need for a process development program to establish improved layup techniques. Consequently, a program was established to determine the maximum number of plies that can be laid up at one time and provide a wrinkle-free overlap laminate after autoclave debulking and curing. Prestaging of the material by vacuum pressure and heat before layup was already in use as a means of attempting to hold

[3] Third Quarterly Research and Development Progress Report for Thiokol 260-Inch Motor Nozzle Program, Riverside, Calif., Rohr Corporation, Space Products Division. 24 April 1964. Report R-1026.

TABLE V

POST-CURE PARAMETERS OF FM-5064 GRAPHITE AND MX-4926 CARBON MATERIALS

Sample Type	Max. Coef. of Thermal Expansion, in./in.	300 F Shrinkage (8 hrs.) in./in.	Net Shrinkage (After Return to 70 F) in./in.	Specific Gravity, g/cc
U.S. Polymeric FM-5064 Graphite, 65-SS-3 Nozzle☆				
As-cured, hydroclave	11.0×10^{-6}	0.00198	0.00083	1.468
Post-cured (48 hrs at 265 F)	6.1×10^{-6}	0.00047	0.00032	1.450
Post-cured (96 hrs at 265 F)	6.1×10^{-6}	0.00029	nil	1.449
Fiberite MX-4926 Carbon, Flat Press Laminate☆☆				
As-cured	4.6×10^{-6}	0.00029	0.00025	1.431
Post-cured (24 hrs at 300 F)	5.3×10^{-6}	0.00011	0.00019	1.406
Post-cured (48 hrs at 300 F)	5.3×10^{-6}	0.00008	nil	1.401
Post-cured (96 hrs at 300 F)	5.3×10^{-6}	nil	nil	1.396

☆ 65-SS-3 midthroat specimens taken tangentially or equivalent to the warp direction of the fabric.

☆☆ Specimens taken parallel to the fill direction.

wrinkling to a minimum. Three 10.7-inch diameter mandrels and one 24-inch diameter mandrel were employed to determine effects of the diameter extremes of the nozzle. Fiberite MX-4600 bidirectional glass laminate was used in the study. Both as-received and prestaging materials were evaluated.

Laminate containing 4, 8, and 12 plies were fabricated on both size mandrels from both the as-received and prestaged material. On some of the prestaged material, a shrinkable release film (2-inch wide Scotchply XP-238) was used to overwrap the glass layups.

The results of the test tended to favor the use of the prestaged bidirectional cloth. However, actual techniques used on the 65-SS-3 motor nozzle also indicated that equally good results could be obtained by using shorter pattern pieces in combination with a debulk after each 8-ply step. The shorter lengths of the fabric pattern probably provided less restraint to the fabric during cure, and circumferential movement was allowed to take place. Detail results of the test are available in Section IV.D of Technical Note No. RPL-TDR-64-101.[4]

(7) Rejection of Aft Throat During Fabrication of 65-SS-3 Nozzle

During fabrication of the components for the 65-SS-3 nozzle, an aft throat was rejected because of radiographic indications that were interpreted as cracks or delaminations. A second aft throat was fabricated, accepted, and used in the nozzle assembly. Further analysis of the rejected throat by sectioning showed that the indications on the X-ray film had been made by the nylon-thread tape-splice pattern and by resin stringers. Experience gained through analysis of this component provides a more satisfactory basis for interpretation of subsequent radiographic film of plastic components. Details of these findings are reported in Report R-1023.[5]

(8) Carbon Tape Storage Problems

During subscale nozzle processing, it was found that properties of carbon tape underwent a change during storage. Upon receipt of the carbon tape material, full inspection of parameters such as flow, volatility, and tack, were performed to assure that the material was within specification limits. The tape was then stored at 35 F up to 10 days and removed from storage for use. Upon removal from storage, the material had virtually no flow and would not tack uniformly, regardless of the heat applied to the material.

As an initial step to solve the problem, which appeared on the surface to be a storage problem, minor modifications were made in the material impregnation process. Slight increases in resin content (toward the upper limit of the specification) and an increase in flow accomplished a leveling-out of

[4] SBR-35.764. 260-Inch Motor Demonstration and 156-Inch Motor Nozzle Test Program, Brunswick, Ga. Thiokol Chemical Corporation, Space Booster Division. 30 June 1964. (Confidential)

[5] Special Events Report, Rejection of Aft Throat for Thiokol Subscale Nozzle No. 2. Riverside, Calif. Rohr Corporation, Space Products Division. 8 April 1964. Report R-1023.

parameters. This was found to be important because the nonimpregnated carbon fabric had a wide degree of variability in several parameters. Examinations of carbon fabric and review of industry specifications for carbon fabric revealed significant variability in four parameters which could affect shelf life and handling characteristics of the pre-preg. These parameters were ash content, pH of the fabric, weight of the fabric, and thickness of the fabric. Table VI shows the original minimum and maximum values permitted for these parameters and the percent difference from minimum to maximum. Table VII shows the revised minimum and maximum values for the four parameters and the revised percent difference from minimum to maximum.

3. Test Results

A varied thickness of elastomeric insulation was provided in the 65-SS-2 entrance cone to obtain information on the erosion resistance of carbon cloth and phenolic resin, different thicknesses of V-44 rubber, and V-61 rubber joint sealer. The design of this entrance section is described in Section IV. A. 1. of this report.

Erosion of each material in the entrance section was uniform with the exception of the areas in line with thickness discontinuity locations. Figure 10 is a view of the entrance cone in the V-44 thickness transition area and shows the more severe erosion caused by the turbulent gas flow. These axially oriented bands of more severe erosion propagated aft of the V-44 termination point. Figure 11 shows the nozzle entrance section and eroded throat, looking through the motor head end PYROGEN port. The 2 1/2-inch thick V-44, flanked by the 1 1/2-inch thickness, appears at the left of the figure, and the exposed carbon tape material appears at the right (light colored area). Erosion depths for the two thicknesses of V-44 and for the V-61 joint sealer are shown as functions of Mach number in Figure 12.

The entrance portion of the 65-SS-3 nozzle was insulated by applying two 180-degree segments of elastomeric materials TI-H704B mastic and ORCO-9250 Buna-N rubber. Figure 13 shows the entrance section of this nozzle after static test. Erosion depths versus Mach numbers for each of the materials are shown in Figure 14. At Mach numbers less than 0.05, performance of TI-H704B was superior to that of ORCO-9250. Performance of ORCO-9250 was better at higher Mach numbers.

With only a few exceptions, performance of the ablative materials met or exceeded predicted performance levels. Average throat erosion was 5.5 mils per second for the 65-SS-2 motor nozzle as compared with the predicted 7.0 mils per second. Some grooving of the throat occurred which was caused by interaction of gases at different Mach numbers coming from the inlet section where the V-44 overlay changed thickness from 2 1/2 to 1 1/2 inches. Throat erosion rate in the grooved areas was approximately 9.25 mils per second. The average erosion rate for the throat of the 65-SS-3 motor nozzle was approximately 6.4 mils per second. Erosion rates of ablative components in the exit sections of the two subscale firings were similar. Figure 15 shows the exit cone for the 65-SS-2 nozzle and Figure 16 is a similar view of the 65-SS-3 nozzle. Figure 17 shows a comparison of the erosion depths throughout the two nozzles and Figures 18 through 21 show comparisons of erosion depth for each material in the two nozzles. Table VIII shows a comparison of the predicted erosion rate with the actual

Figure 10 - Erosion Caused by Turbulent "Rolling" Gas Waves, 65-SS-2 Motor

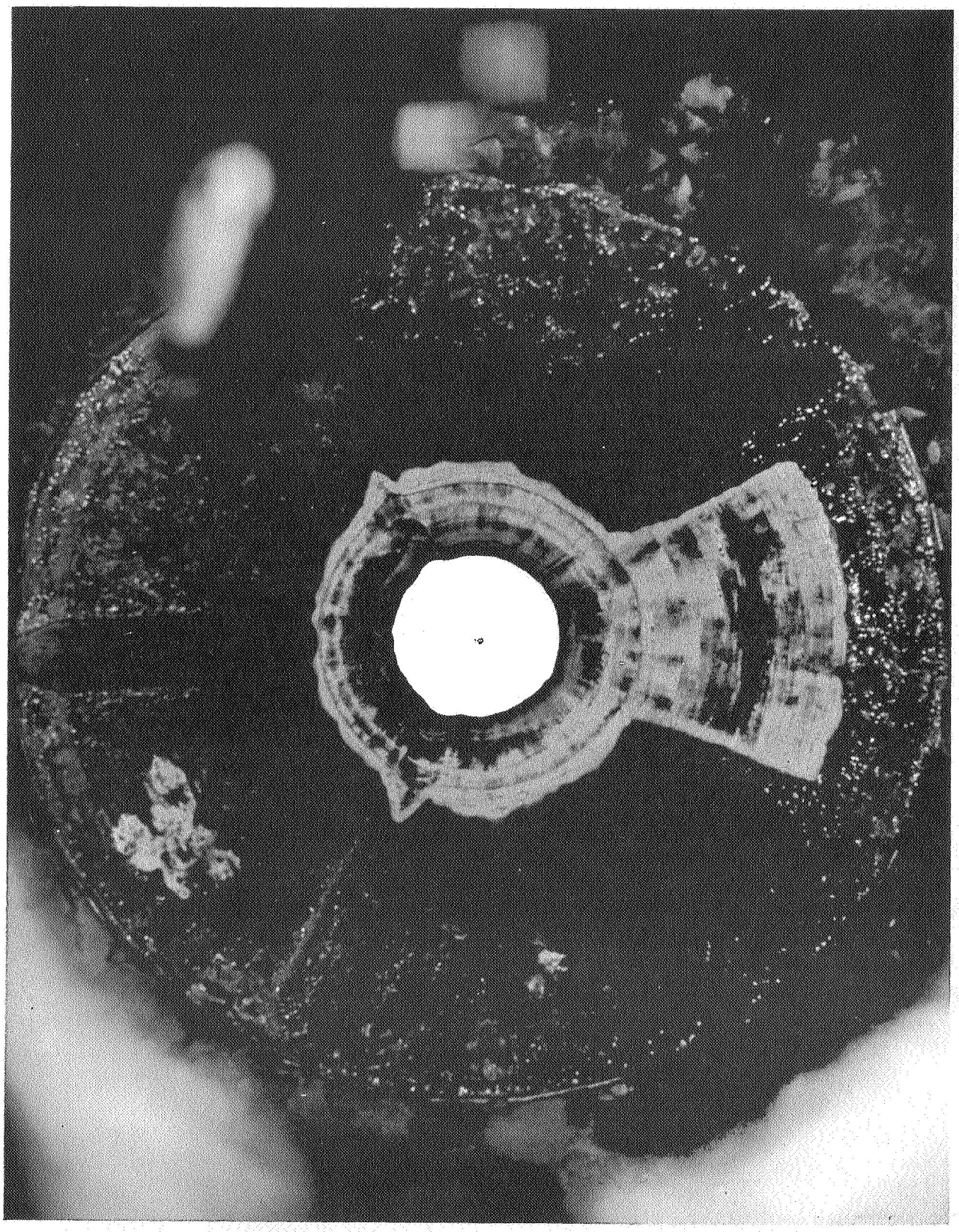

Figure 11 - Nozzle Entrance Section and Eroded Throat, 65-SS-2 Motor

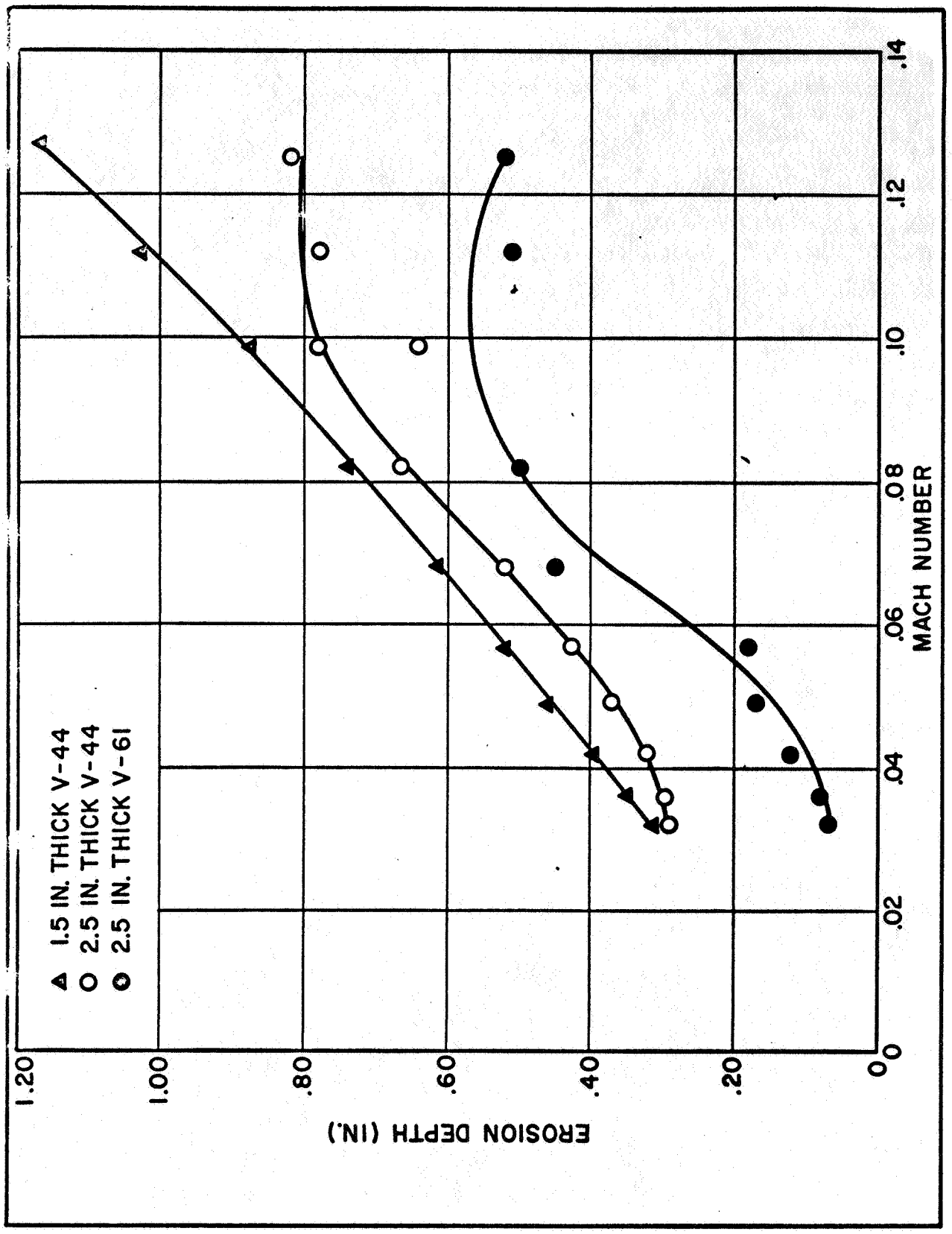

Figure 12 - Erosion Depths of V-44 Rubber and V-61 Sealer, 65-SS-2 Motor

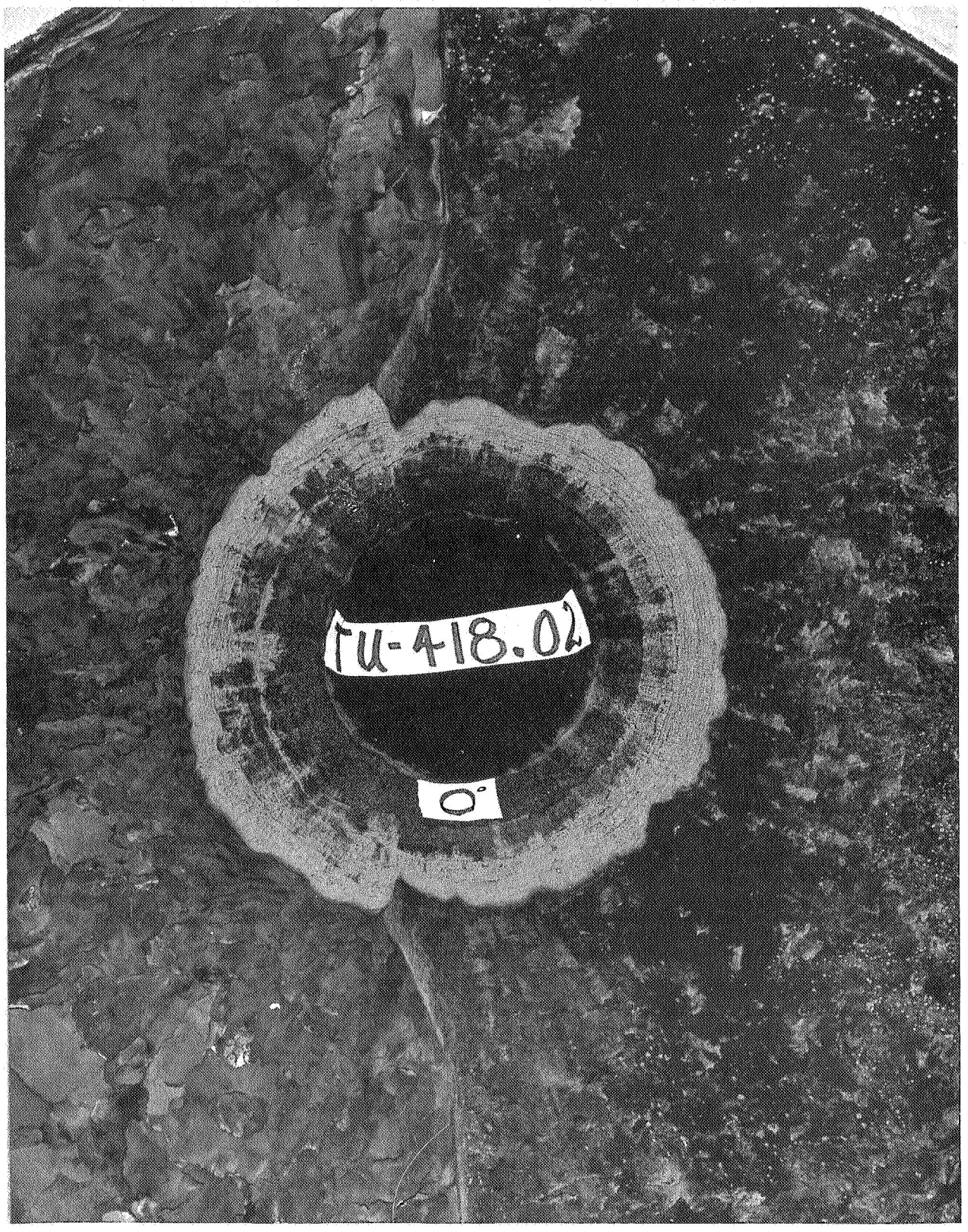

Figure 13 - Nozzle Entrance Cone after Static Test of 65-SS-3 Motor

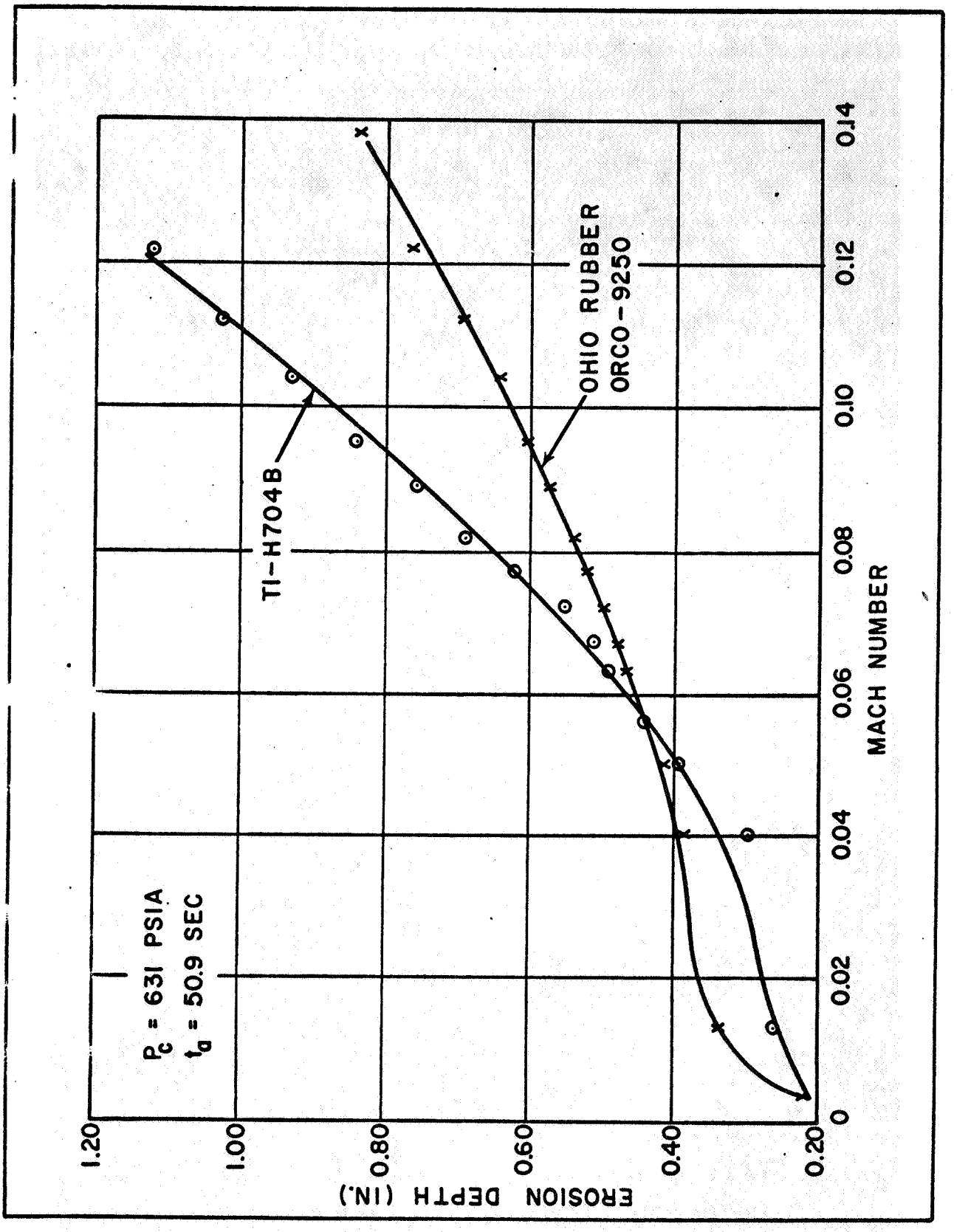

Figure 14 - Comparison of Average Erosion Data from Mastic and Asbestos Silica-Filled Buna-N Insulation in 65-SS-3 Motor

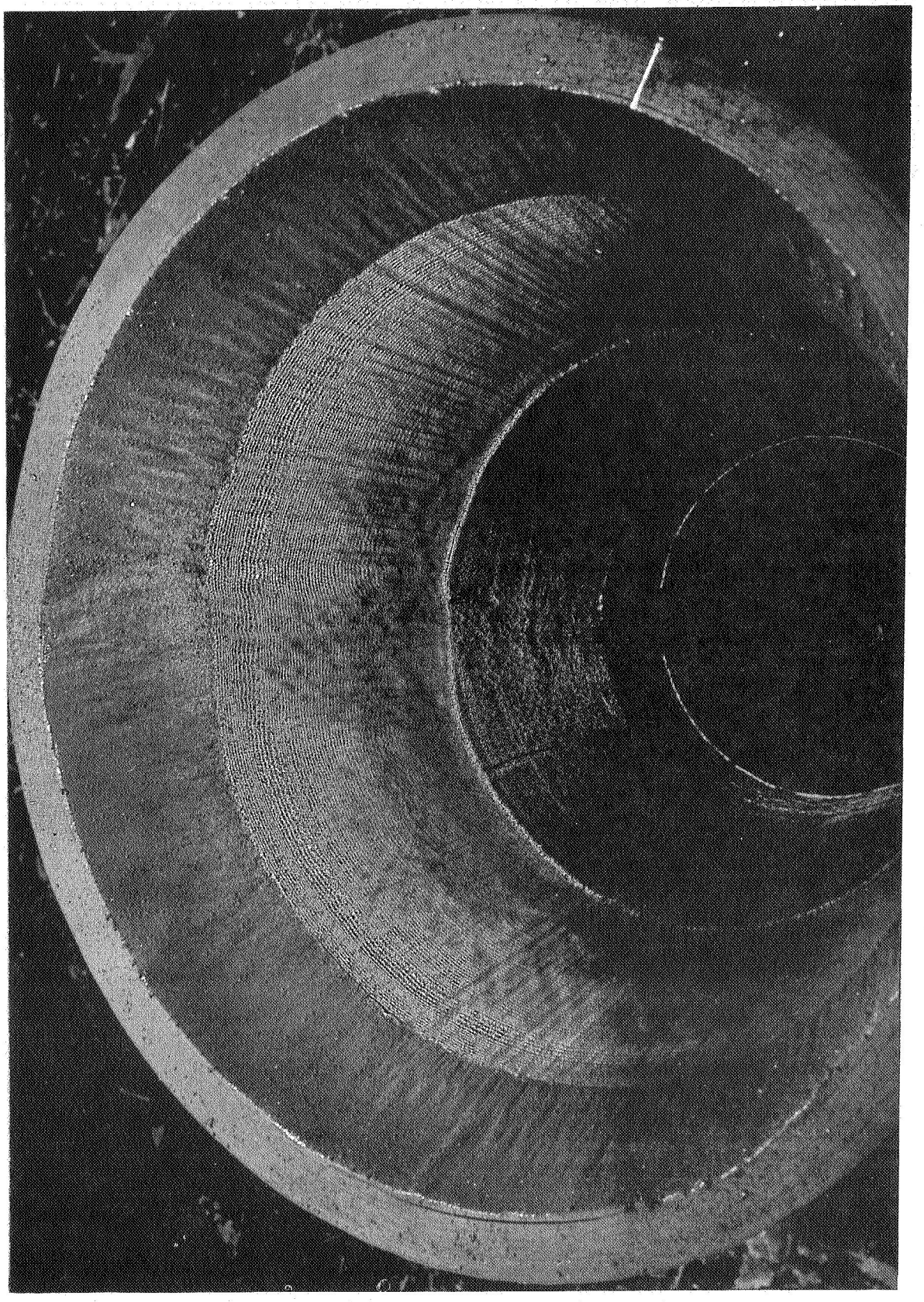

Figure 15 Nozzle Exit Cone after Firing, 65-SS-2 Motor

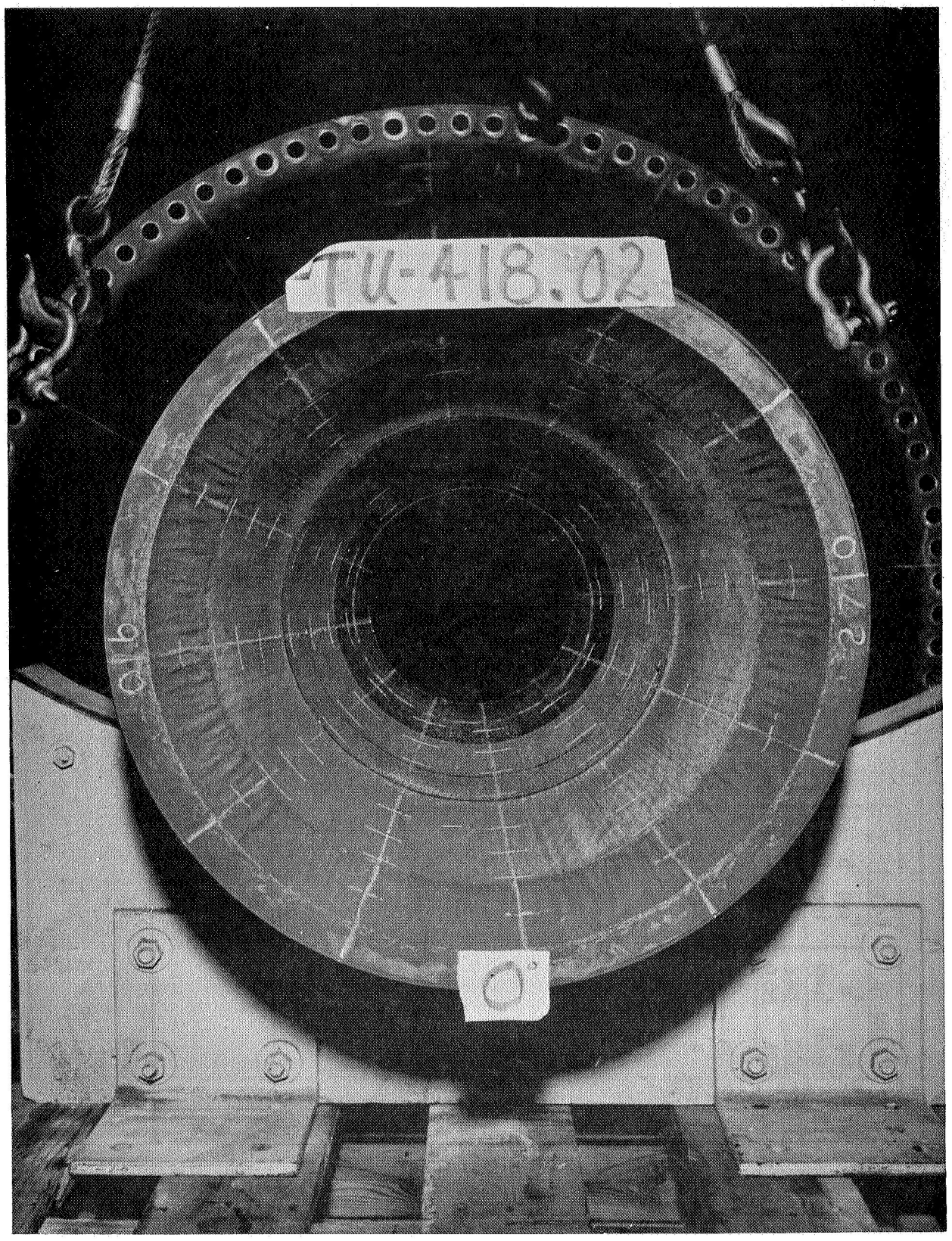

Figure 16 - Nozzle Exit Cone after Static Test of 65-SS-3 Motor

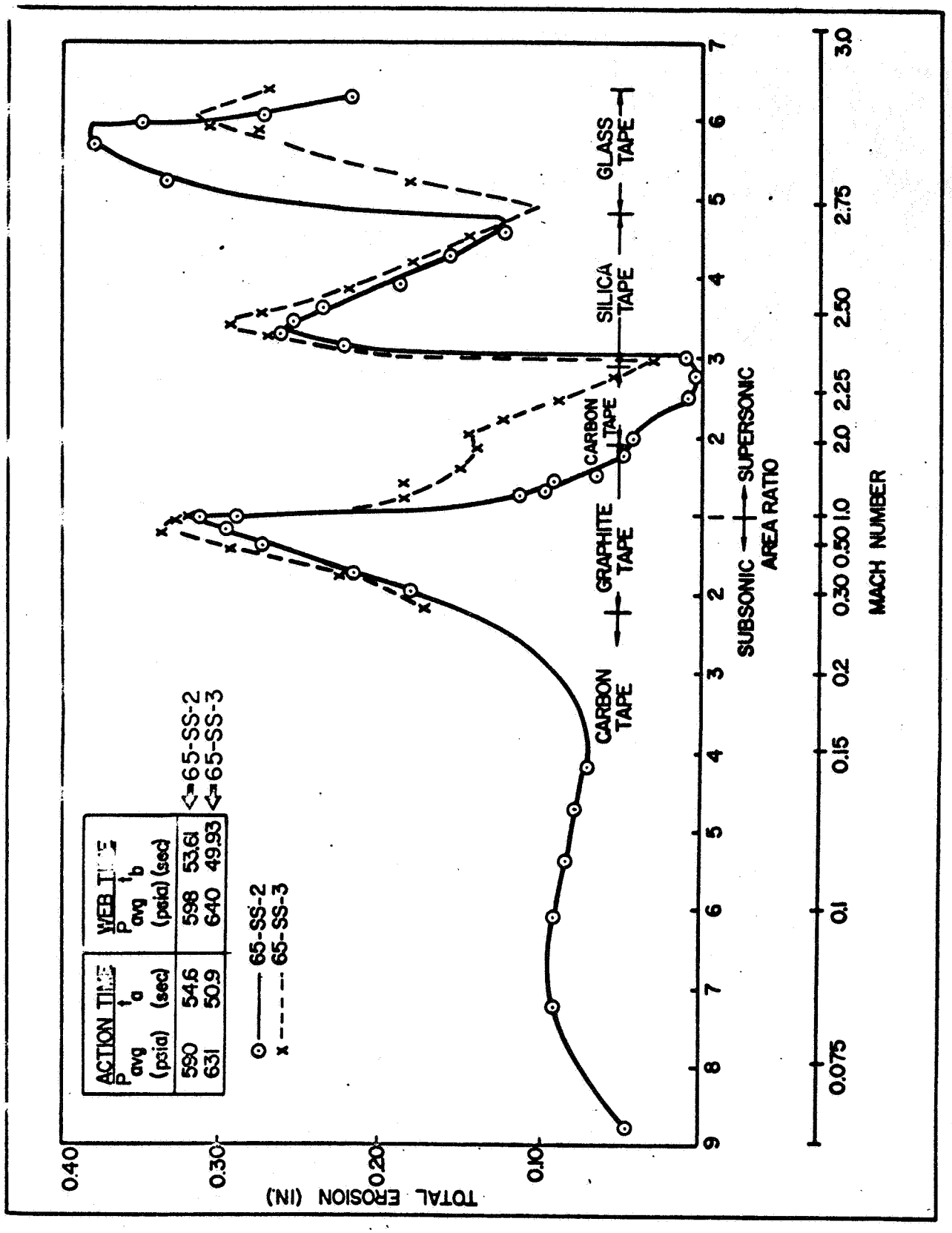

Figure 17 - Average Erosion Data for 65-SS-2 and 65-SS-3 Nozzle Plastic Components

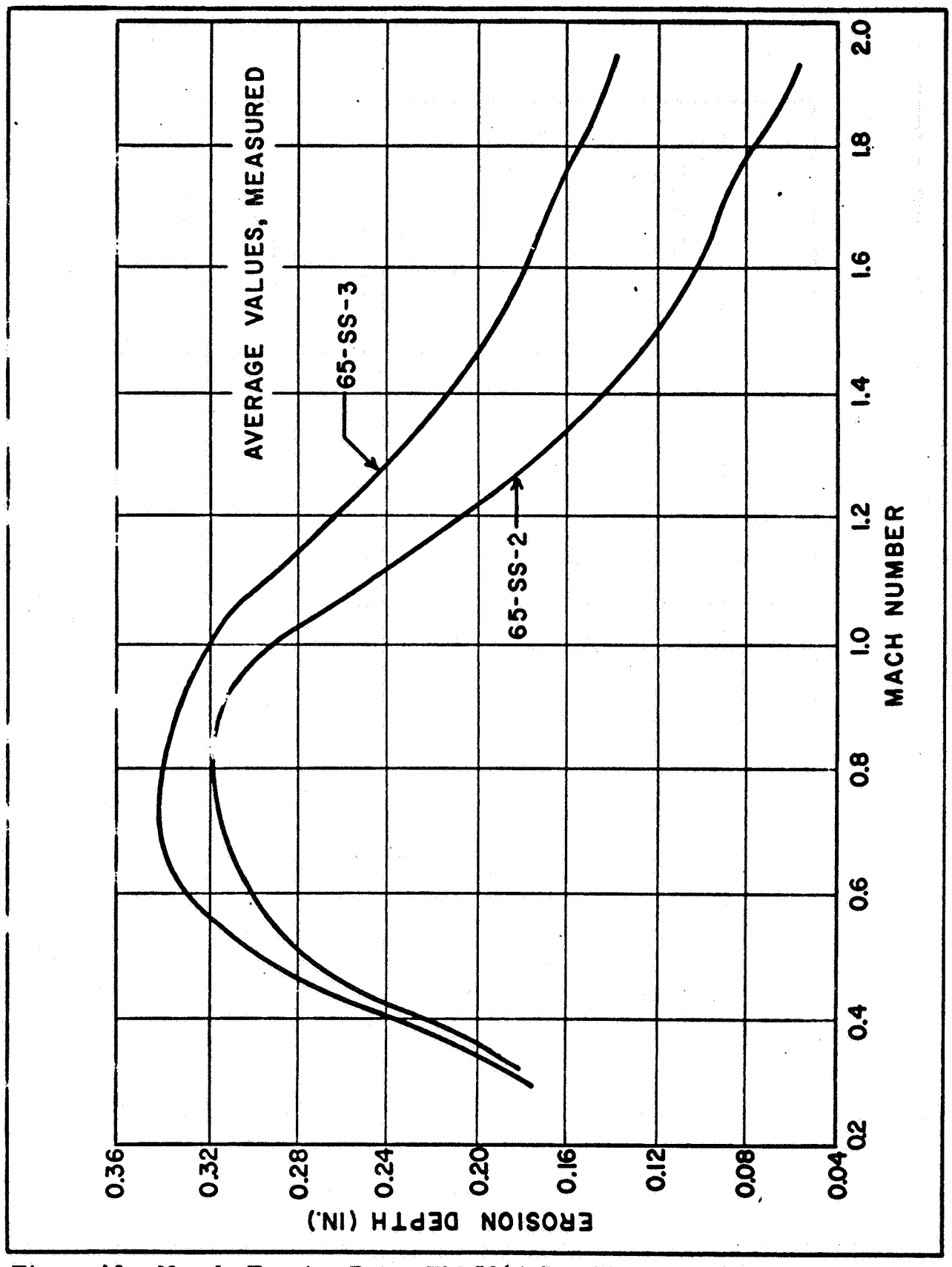

Figure 18 - Nozzle Erosion Data, FM-5064 Graphite Tape

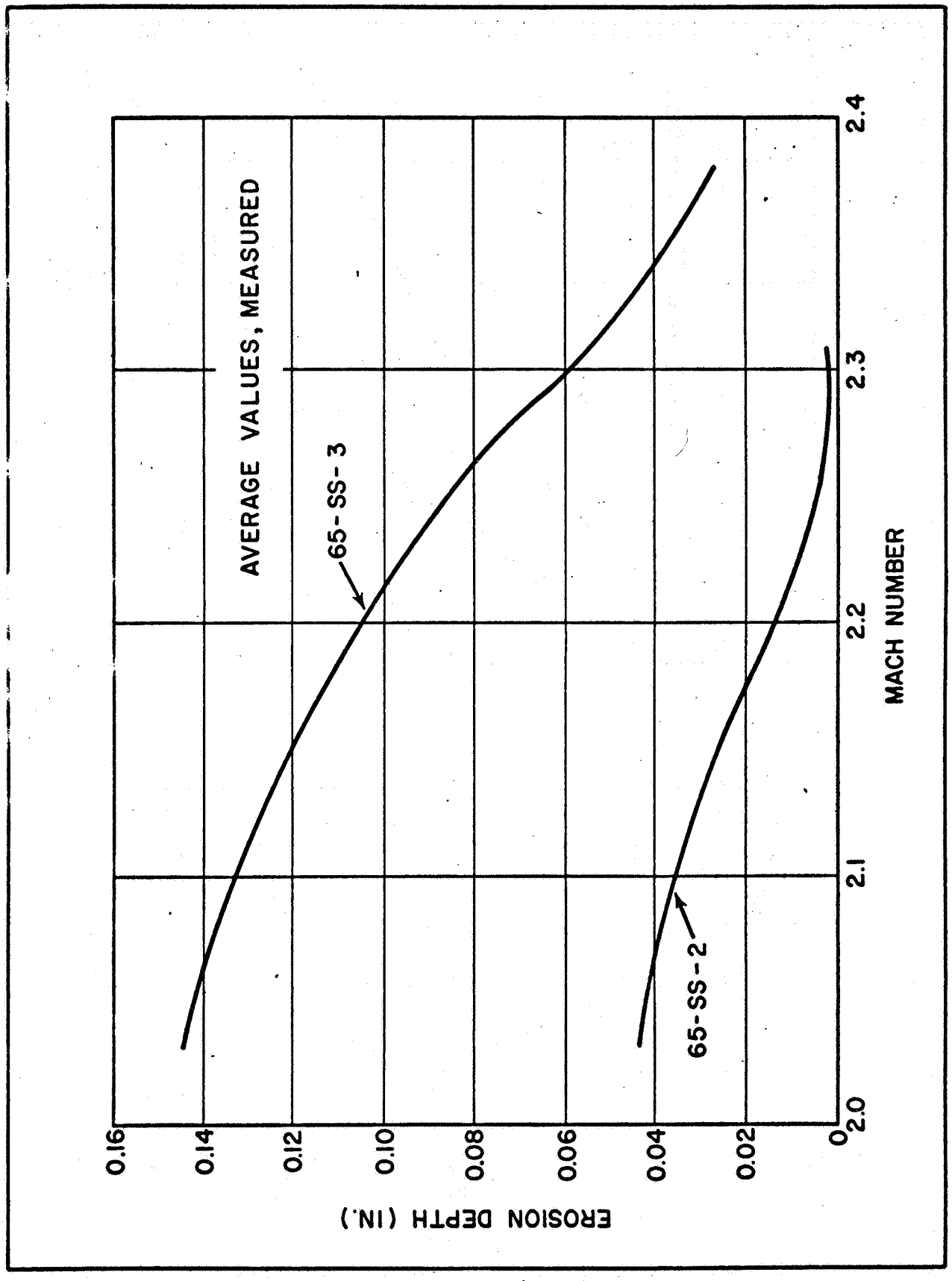

Figure 19 - Nozzle Erosion Data, MX-4926 Carbon Tape

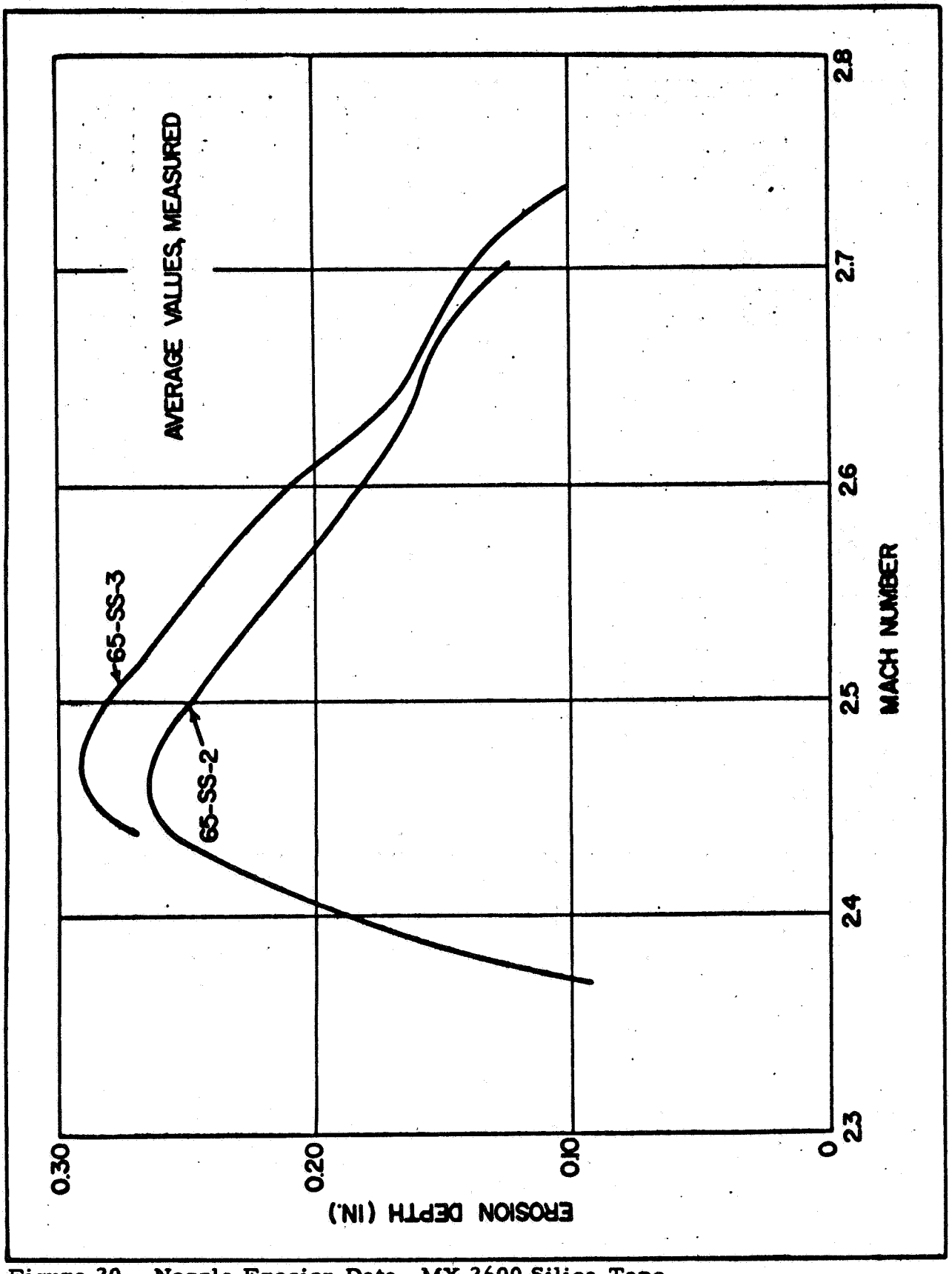

Figure 20 - Nozzle Erosion Data, MX-2600 Silica Tape

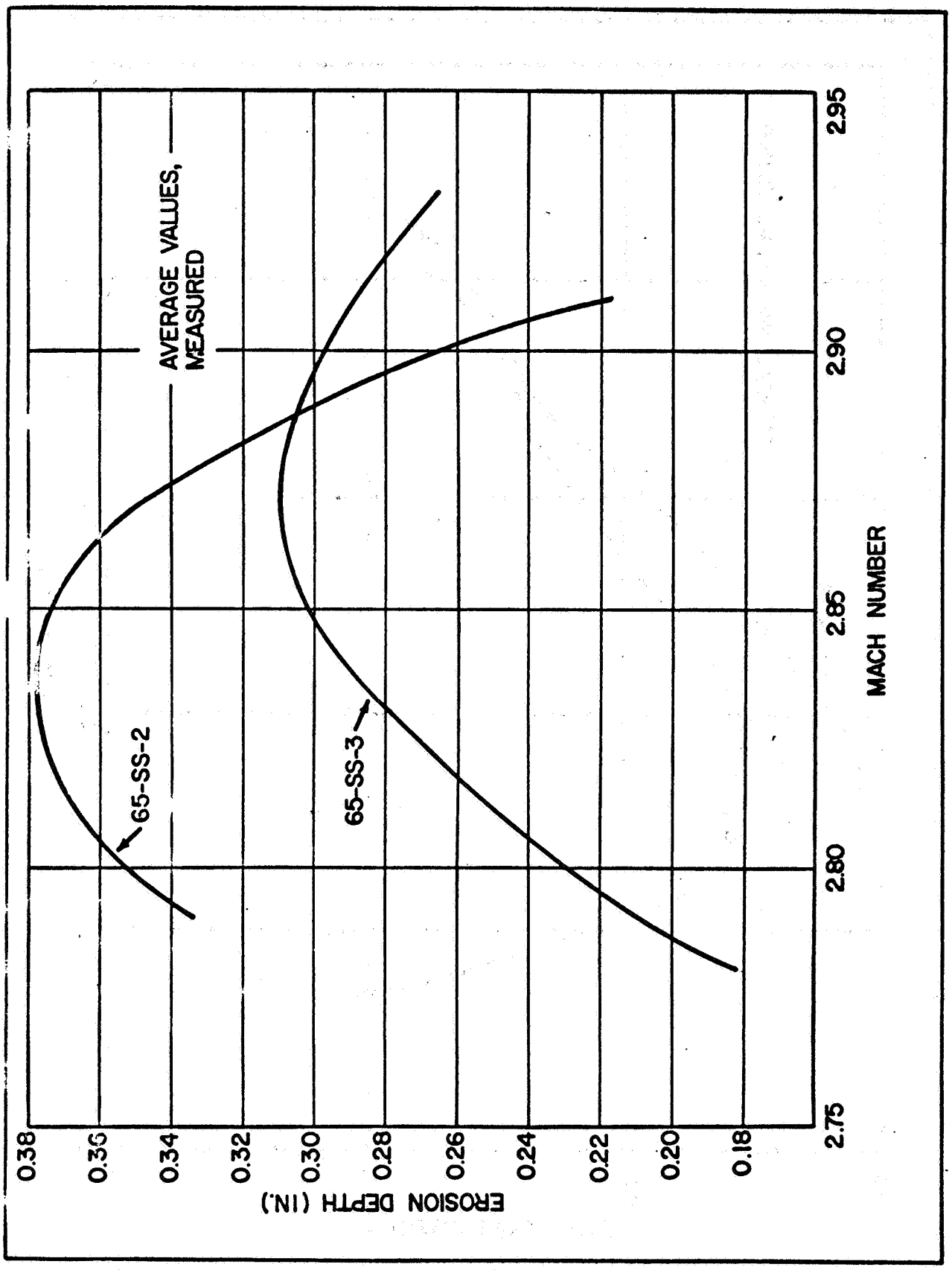

Figure 21 - Nozzle Erosion Data, MX-4600 Glass Tape

TABLE VI

ORIGINAL VARIATIONS IN CARBON FABRIC
BASIC PARAMETERS

Parameter	Value		Percent Difference*
	Minimum	Maximum	
Ash Content, weight %	--	1.2	--
pH	6.5	10.0	54
Weight, oz./yard^2	7.0	9.0	28
Thickness, in.	0.017	0.023	35

TABLE VII

REVISED LIMITS FOR CARBON FABRIC
BASIC PARAMETERS

Parameter	Value		Percent Difference*
	Minimum	Maximum	
Ash Content, weight %	--	0.5	--
pH	8.0	10.0	25
Weight, oz./yard^2	8.0	9.0	13
Thickness, in.	0.016	0.020	25

* Minimum to maximum

TABLE VIII

PREDICTED VERSUS ACTUAL EROSION RATES FOR THE 65-SS-2 AND 65-SS-3 ABLATIVES

Material	Mach No.	Average Erosion Rate, mils/sec		
		Predicted	65-SS-2	65-SS-3
FM-5063	0.15	4.1	1.5	Note 1
FM-5064	0.30	4.8	3.4	3.6
	0.60	5.9	5.6	6.6
	1.0	7.0	5.5	6.4
	1.6	5.0	1.9	3.6
MX-4926	2.1	4.3	0.7	2.7
MX-2600	2.5	5.3	4.7	5.6
MX-4600	2.8	4.5	6.5	4.6
	2.9	4.1	5.0	6.0

NOTES: 1. The small ring of carbon in the entrance section of 65-SS-3 was covered with elastomeric insulation.

erosion rate from the two nozzles, and Table IX shows a comparison of predicted and actual char depths for the two nozzles. It can be seen that actual char thicknesses are equal to or less than predicted char thicknesses. A series of delaminations was found in the carbon tape sections, but were of shallow depth and typical of post-firing shrinkages occurring during cooldown. No delaminations occurred in the other ablative materials.

Of the four ablative-to-ablative joints in the 65-SS-2 nozzle, two were filled with phenolic resin cured at 275 to 300 F and two were filled with Epon 913 epoxy adhesive with a 5-percent Cab-O-Sil filler as a thixotropic agent. Those joints filled with Epon 913 showed degradation of the bond line in the heat-affected areas. Those joints filled with phenolic resin performed satisfactorily. Based on these results, zinc chromate putty was used in the mid-throat-to-aft throat joint of the 65-SS-3 motor nozzle for performance evaluation. Performance was entirely satisfactory, as shown by the existence of unaffected material at a depth of 0.06 inch below the surface of the nozzle. There was no indication of any tendency for the gas stream to draw out the putty.

After a problem had been encountered with temperature-cured adhesive on the 65-SS-2 forward throat, Epon 913 ambient curing adhesive was used to bond the remaining ablatives for this nozzle to the steel shell. In the entrance cone region, this adhesive separated from the steel shell, permitting the unbonded entrance cone to remain on the motor case rather than with the steel shell at motor disassembly. This separation was attributed to the fact that the shell had not been grit blasted in this area.

Epon 913 was also used on 65-SS-3 between the ablatives and the steel shell after sand blasting. It was found necessary to heat the 65-SS-3 nozzle to 400 F to achieve ablative separation from the shell.

a. Conclusions

Performance of the 65-SS-2 nozzle was generally satisfactory and verified the materials and design concept adequacy. Ablation performance was equal to or superior to design predictions except for areas exposed to high turbulence and except for the MX-4600 glass tape section of the exit cone. Thickness discontinuities in the elastomeric insulation of the entrance section which caused the turbulence were not typical of the full-scale nozzles nor of the configuration of the 65-SS-3 nozzle. The only change made in the full-scale nozzle ablative materials as a result of the subscale test was the deletion of MX-4600 glass tape as an ablative material; MX-2600 silica material was substituted. Because of schedule commitments, this change was not imposed on the 65-SS-3 nozzle.

Based on 65-SS-2 data, a change of joint materials was concluded to be necessary to effect a more reliable seal for ablative-to-ablative joints. Analyses of fabrication requirements for full-scale nozzles showed that phenolic resin, though performing quite well, could not be practically used. Zinc chromate putty was used and evaluated in one joint of the 65-SS-3 nozzle because of experience with it as a joint filler in other programs.

Grit blasting of the steel shell and better protection of the surface prior to bonding solved the problem of bonding encountered on 65-SS-2.

TABLE IX

PREDICTED VERSUS ACTUAL CHAR THICKNESSES
FOR THE 65-SS-2 and 65-SS-3 ABLATIVES

Material	Area Ratio*	Average Char Thickness, inch		
		Predicted	65-SS-2	65-SS-3
FM-5063	-9.0	0.55	0.51	**
Carbon	-5.0	0.55	0.50	**
FM-5064	-3.0	0.67	0.60	***
Graphite	-2.0	0.67	0.61	0.56
	1.0	0.55	0.52	0.50
	1.5	0.49	0.54	0.50
MX-4926				
Carbon	2.5	0.32	0.25	0.32
MX-2600				
Silica	3.5	0.27	0.18	0.17
MX-4600				
Glass	5.5	0.14	0.10	0.09

* Minus sign designates convergent section.

** FM-5063 not exposed for full duration.

*** FM-5063 used in this location on 65-SS-3; not exposed for full duration.

Successful performance of the 65-SS-3 nozzle reconfirmed the adequacy of materials, basic fabrication processes, and the design concept selected for use in the 156-2C-1 nozzle and in the 260-SL-1 nozzle. Changes in material and processes incorporated after static test of the 65-SS-2 nozzle were shown to be satisfactory and indicated suitability for use in full-scale nozzles. No additional changes in design, materials, or processes were found to be required based on performance of the 65-SS-3 nozzle.

B. CASE AND CLOSURE

Motors 65-SS-2 and -3 utilized heavyweight TU-190 chambers that had previously been fired in the MINUTEMAN program. These chambers were made by Kaiser Corporation from low carbon alloy (T-1) steel and have a nominal wall thickness of 0.50 inch. They had been hydrotested, and therefore only required cleaning for use in this program. Cleaning (degreasing) was accomplished by the standard techniques of spray and hand cleaning with trichloroethylene. New closures were made by E.W. Bliss Company to accommodate the single nozzle configuration. Minimum wall thickness of the closures is 2.0 inches. Table X details pertinent chamber and closure information.

C. PROPELLANT

1. Type

The propellant loaded into the 65-SS-2 and 65-SS-3 motors was TP-H8163, which was developed for use in the 156-2C-1, 260-SL-1, and 260-SL-2 motors. This propellant was 85% solids loaded.

Propellant tailoring had been completed at the time of subscale motor loading. Therefore, only a raw material standardization was required for the propellant. Development size propellant mixes were prepared to standardize raw materials so that the proper polymer-curing agent ratio and ground-to-unground oxidizer ratio could be selected. Physical property data measured on mixes manufactured to load the two motors are provided in Table XI. These data are consistent with that generated during the propellant development and 156-2C-1 motor manufacture.

2. Casting

Propellant for the subscale motors was manufactured in 300-gallon vertical mixers and deaerated directly into the motor cases using a vacuum casting technique. After casting, the propellant was cured for a minimum of 7 days at 135 F.

TABLE X

CHAMBER-CLOSURE GEOMETRY, 65-SS-2 AND 65-SS-3

Dimension/Property	Parameter
Case Nominal Outside Diameter (in.)	66.25
Closure (conical), Length (in.)	11.35
Cylindrical Section Length (in.)	43.8
Safety Factor on Yield Strength (case)	1.80
Yield Strength of Case Material (psi)	90,000
Ultimate Strength of Case Material (psi)	105,000

TABLE XI

PHYSICAL PROPERTIES OF PROPELLANT LOADED IN 65-SS-2 AND 65-SS-3 MOTORS

Motor and Mixes	Properties			
	Modulus, psi	Stress, psi	Ult. Strain, in./in.	Strain at Max. Stress, in./in.
Mix 1, 65-SS-2	490	103	0.39	0.32
Mix 2, 65-SS-2	420	94	0.40	0.31
Mix 3, 65-SS-2	500	100	0.36	0.30
Mix 1, 65-SS-3	450	96	0.40	0.31
Mix 2, 65-SS-3	410	94	0.40	0.33
Mix 3, 65-SS-3	566	99	0.29	0.25

NOTE: Mix size was 300 gallons.

D. LINER AND INSULATION

1. Type

The liner and insulation materials used in the 65-SS-2 and 65-SS-3 motors were the same as those developed for use in the 156-2C-1, 260-SL-1, and 260-SL-2 motors. The composition of these materials (TL-H714A liner and TI-H704B insulation) is given in Table XII. All raw materials purchased for use were standardized according to Space Booster Division specifications and were acceptable. Typical tensile and bond properties are summarized below.

TI-H704B Insulation

Tensile Properties	
Net Stress	187 psi
Net Strain	2.27 in./in.
Adhesion Properties	
Insulation to steel	285 psi
Insulation to liner	89 psi
Peel Properties	
Liner to insulation	27 pli

TL-H714A Liner

Tensile Properties	
Net Stress	319 psi
Net Strain	8.70 in./in.
Adhesion Properties	
Liner to propellant	115 psi
Peel Properties	
Liner to propellant	28 pli

2. Application

The TI-H704B insulation was hand-troweled into the two motors. A pneumatic tapping tool was then used to spread and smooth the insulation after it was applied to the case. However, a completely smooth surface was difficult to obtain with the tapping tool. The insulation was applied in all areas in thicknesses greater than required by design. The insulation material was not vacuum mixed, but was slit deaerated prior to application on the case. Isolated subsurface voids were detected in strips of insulation removed from the motor.

A 10-inch deep flap was built into the aft end of each motor to relieve stress singularities at the aft grain-case juncture. The flap was composed of polyethylene, fiberglass cloth, and TI-H704B insulation. A sheet of polyethylene was inserted between two layers of fiberglass cloth and the lower layer of

TABLE XII

MATERIAL COMPOSITIONS- LINER AND INSULATION

TL-H714A Liner

Raw Material	Weight Percent
HC Polymer (HX-740, HX-760)[2] [1]	70±5
Carbon Black	25±5

TI-H704B Insulation

Raw Material	Weight Percent
HC Polymer (HX-740, HX-760)[3] [1]	45±2
Carbon Black	15
Asbestos	30±2
Diammonium Phosphate	10

NOTES:
1. Binder composition subject to standardization.
2. 2/1 equivalent ratio.
3. 6/1 equivalent ratio.

cloth was bonded into the case with freshly prepared insulation. The outer side of the second layer was also then coated with insulation. Because of poor wetting properties of the insulation material, it was very difficult to apply the material on to the cloth and, as a result, several wrinkles were apparent. The wrinkles, however, did not affect performance or integrity. Insulation in the flap region was subjected to 8 hours cure at 135 F prior to applying the liner.

In addition to being evaluated in the interior of the cases, the TI-H704B was further evaluated in the forward section of the nozzle of the 65-SS-3 motor. One half of the forward section (180°) was insulated with TI-H704B insulation and the remaining portion with a standard commercial asbestos-filled Buna-N insulation. The TI-H704B insulation was again applied by hand trowelling.

The liner composition used contained 70 percent binder and 30 percent carbon black. This liner was sling applied by being fed into a rapidly rotating disc having a narrow peripheral slot through which small globules of liner passed at high speed. Impact with the case wall helped to spread the liner.

3. Performance

Results of post-firing tests of insulation in the 65-inch motor firings were somewhat inconclusive in that some of the post-fire thicknesses exceeded the prefire thicknesses at the same points of measurements. The occurrence is attributed in part to the tendency of the insulation to swell when heated. It was also difficult to record the prefire and post-fire measurements at exactly the same point. Nevertheless, the performance of the insulation was satisfactory. In addition to being evaluated in the interior of the cases, the TI-H704B insulation was further evaluated in the forward section (adapter) of the nozzle of the 65-SS-3 motor. The post-firing examination showed that the TI-H704B insulation had better erosion resistance at the lower Mach numbers, 0.056 and below, and the Buna-N material was only slightly superior at the higher Mach numbers (see Figure 14). Based on these results, TI-H704B insulation was selected, rather than the asbestos-filled Buna-N insulation, for the adapter sections of the 260-SL-1 and 260-SL-2 motors.

E. IGNITION SYSTEM

Ignition of the 65-SS-2 and 65-SS-3 motors was accomplished with a forward mounted PYROGEN ignition system designated TU-P137. This unit was previously used to ignite three major subscale test motors during the MINUTEMAN development program. The PYROGEN ignition system consisted of a fiberglass case with a case-bonded grain (Drawing U3952) and an initiator assembly which contained one U.S. Flare 107-A squib and a booster charge of boron potassium nitrate pellets (Drawing U6797). The grain contained 1.75 pounds of TP-E8035 propellant and had an internally burning five-point star configuration.

The TU-P137 PYROGEN ignition system ignited the 65-SS-2 and 65-SS-3 grains within the expected limits. The time to 90 percent maximum chamber pressure for the igniter was 0.014 and 0.016 second respectively for the two tests. The maximum pressure for both tests was 964 psia. The motor ignition delay, time to 10 percent maximum motor chamber pressure, was 0.127 second for the 65-SS-2 motor and 0.225 second for the 65-SS-3 motor.

F. MOTOR FINISHING

After propellant cure the motors were cooled down to a temperature below 100 F and the core was pulled. The core was pulled in both motors without any difficulty and the internal grain was inspected. No defects were noted. While the motors were in the vertical position, the polyethylene sheets were removed from the aft flap and the gap was filled with a flap filler compound (TA-G701B). The TA-G701B was allowed to cure for 72 hours at ambient temperature prior to placing the motors in a vertical position.

Prior to the assembly of the nozzle to the loaded motor, the joint area where the carbon and/or elastomeric insulation in the nozzle would mate with the TI-H704B in the adapter was filled with zinc chromate putty. The putty served as an erosive resistant joint seal.

V. INTERNAL BALLISTICS

The item of major ballistic significance resulting from the subscale motor program was reference specific impulse (I_{sp}). The 65-SS-2 and -3 motors yielded reference I_{sp} values of 244.8 and 245.1 lbf-sec/lbm, respectively.

Ballistic performance of 65-SS-2 and -3 is shown in Table XIII, and thrust and pressure versus time traces are shown in Figures 22 and 23.

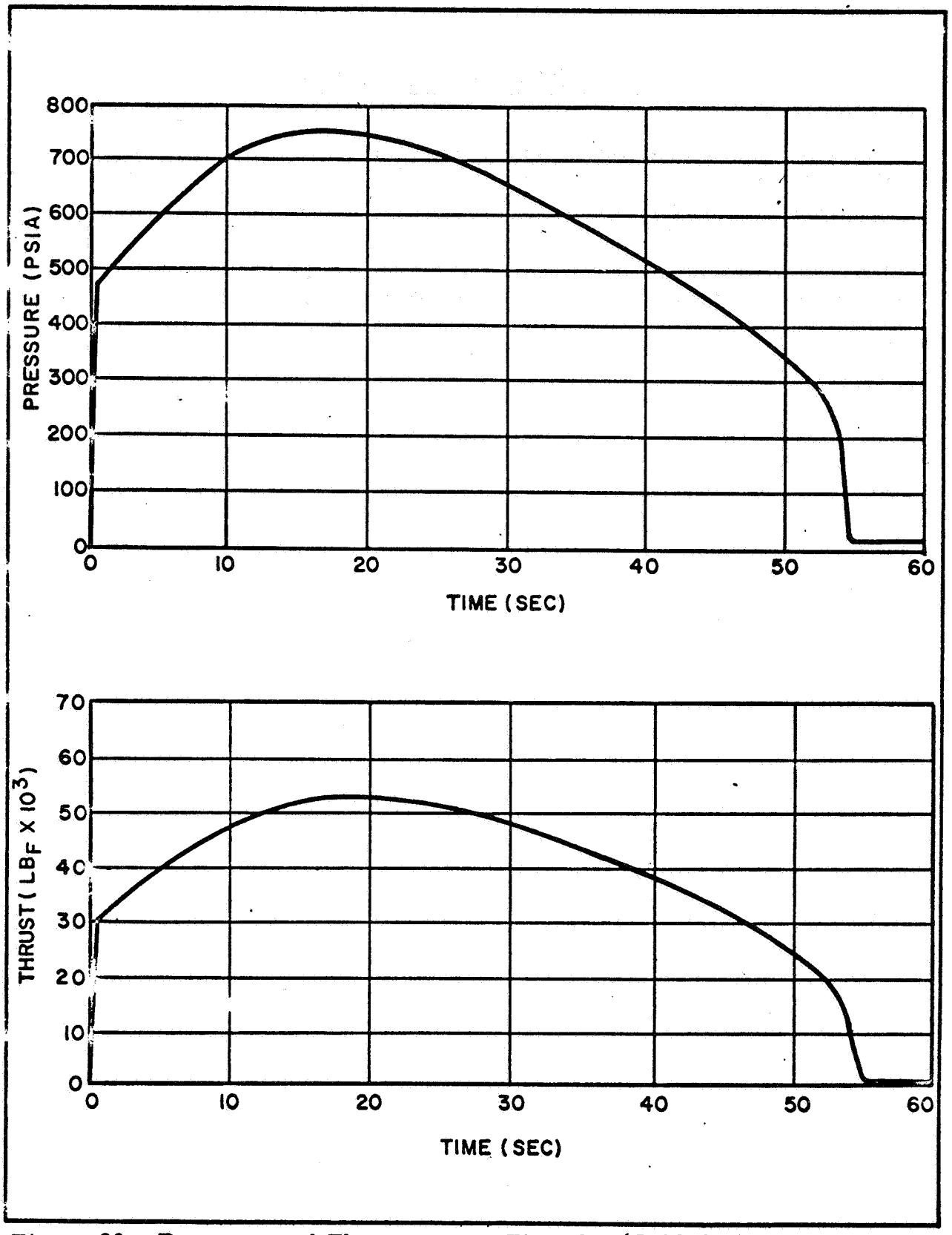

Figure 22 - Pressure and Thrust versus Time for 65-SS-2 Motor

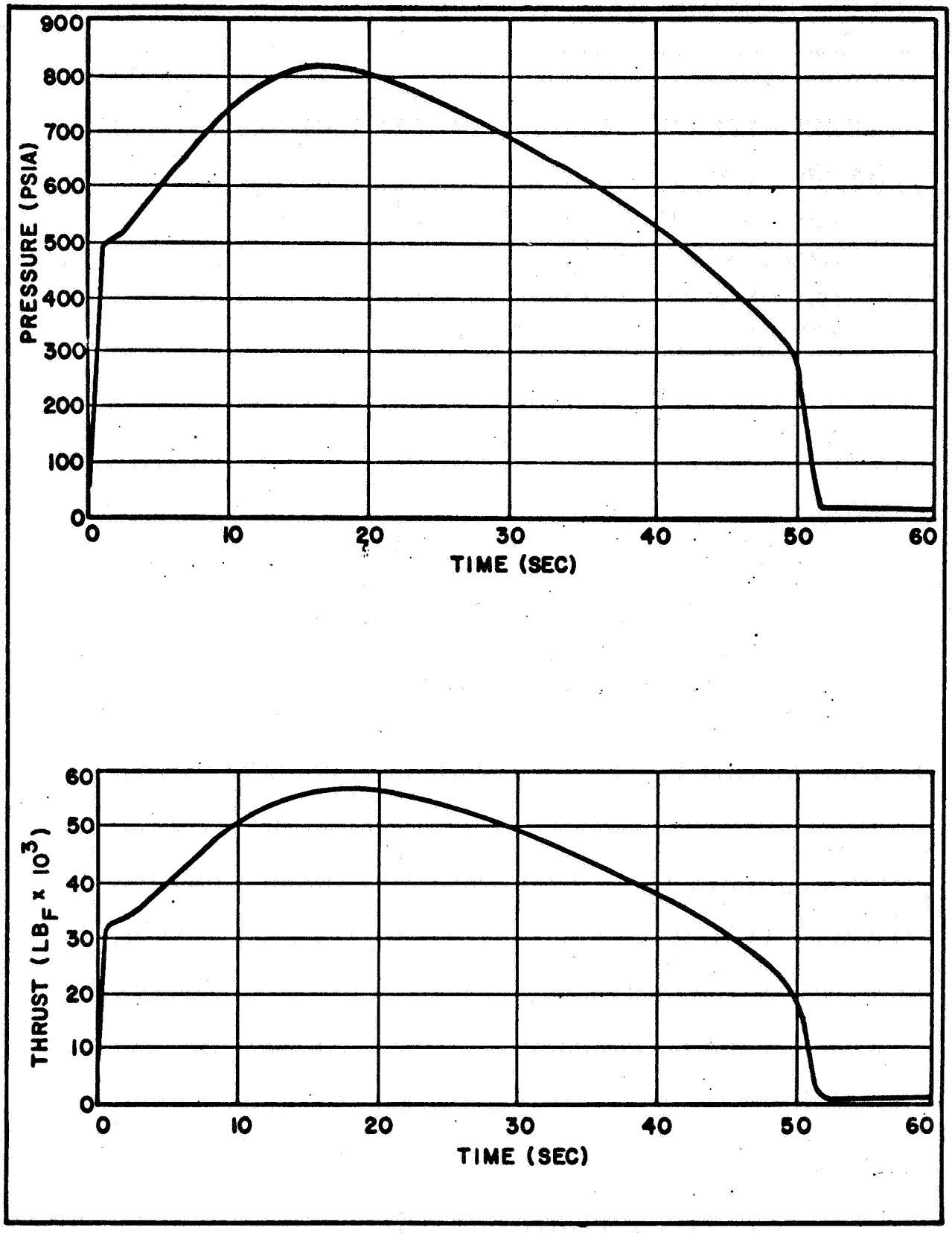

Figure 23 - Pressure and Thrust versus Time for 65-SS-3 Motor

TABLE XIII

BALLISTIC PERFORMANCE, 65-SS-2 AND 65-SS-3

	TU-418.01 65-SS-2	TU-418.02 65-SS-3
Test Conditions		
Conditioning Time, hrs	117	60
Average Grain Temp., F	81 ± 1	77.6 ± 1
Ambient Temp. at Test, F	18	60
Barometric Pressure at Test, psia	12.6	12.3
PYROGEN Data		
t_{cp}, sec (time to 90 percent p_{max})	0.014	0.016
p_{max}, psia	964	964
Ignition Data		
t_d, sec (time to 10 percent p_{max})	0.127	0.225
Action Time Data		
t_a, sec (time from 10 percent p_{max} on ignition to 10 percent on decay)	54.60	50.90
Pdt, psia-sec	32,230	32,114
$\overline{P}_c$, psia	590	631
I, lbf-sec	2,258,000	2,247,000
$\overline{F}_a$, lbf	41,360	44,140
W_p useful, lbm☆	9,600	9,456
Isp_{del}, lb-sec/lb	235.2	237.6
Web Time Data		
t_b, sec	53.61	49.93
p_{max}, psia	761	822
$\overline{P}_c$, psia	598	640
F_{max}, lbf	53,380	57,230
$\overline{F}_b$, lbf	41,930	44,780
$\overline{r}_b$, in/sec	0.427	0.459
Pdt, psia-sec	32,070	31,940
Reference Specific Impulse, lb-sec/lb	244.8	245.3

☆Assumed to be equal to W_p total

VI. STATIC TESTING

The subscale motors were roller supported and tested in a horizontal, single component test stand (see Figure 24). The motors were conditioned at 80 ± 10 F. The humidity and temperature of the motor environments were continuously recorded from the time of propellant casting until T-1 hour at an accuracy of ±10 percent relative humidity and ±10 F temperature. A special quench system was actuated as soon as possible after tailoff to prevent excess burning of the nozzle components.

All instrumentation was continuously recorded for the duration of the tests. The following types of instrumentation were installed in accordance with Thiokol drawing 1S36001B to obtain the required data.

1. Pressure gages -

   Igniter: 2 gages, 0-1500 psia, ±0.5 percent
   Chamber: 3 gages, 0-900 psia, ±0.5 percent

2. Thrust gages - 3 gages, 0-70,000 lbs, ±3.0 percent

3. Accelerometers - 6 gages, 0-20g (10kc), ±10.0 percent

4. Strain gages - 12 gages, 0-0.005 in./in., ±5.0 percent

5. Temperature gages - 22 gages, 0-1000 F, ±5.0 percent

Motion pictures of the static tests were taken from a location having an unobstructed view. The coverage provided was as follows:

1. Two slow speed cameras of vicinity of nozzle and closure.

2. One sequence camera of the vicinity of nozzle and closure.

3. Two high speed cameras, 1000 frames per second, in sequence, covering vicinity of nozzle and closure.

Black and white still photographs were taken as follows:

1. Nozzle exit cone prior to and following static test.

2. Motor in test stand showing instrumentation prior to and following static test.

3. Inside of case from igniter port showing nozzle entrance cone and aft closure following static test.

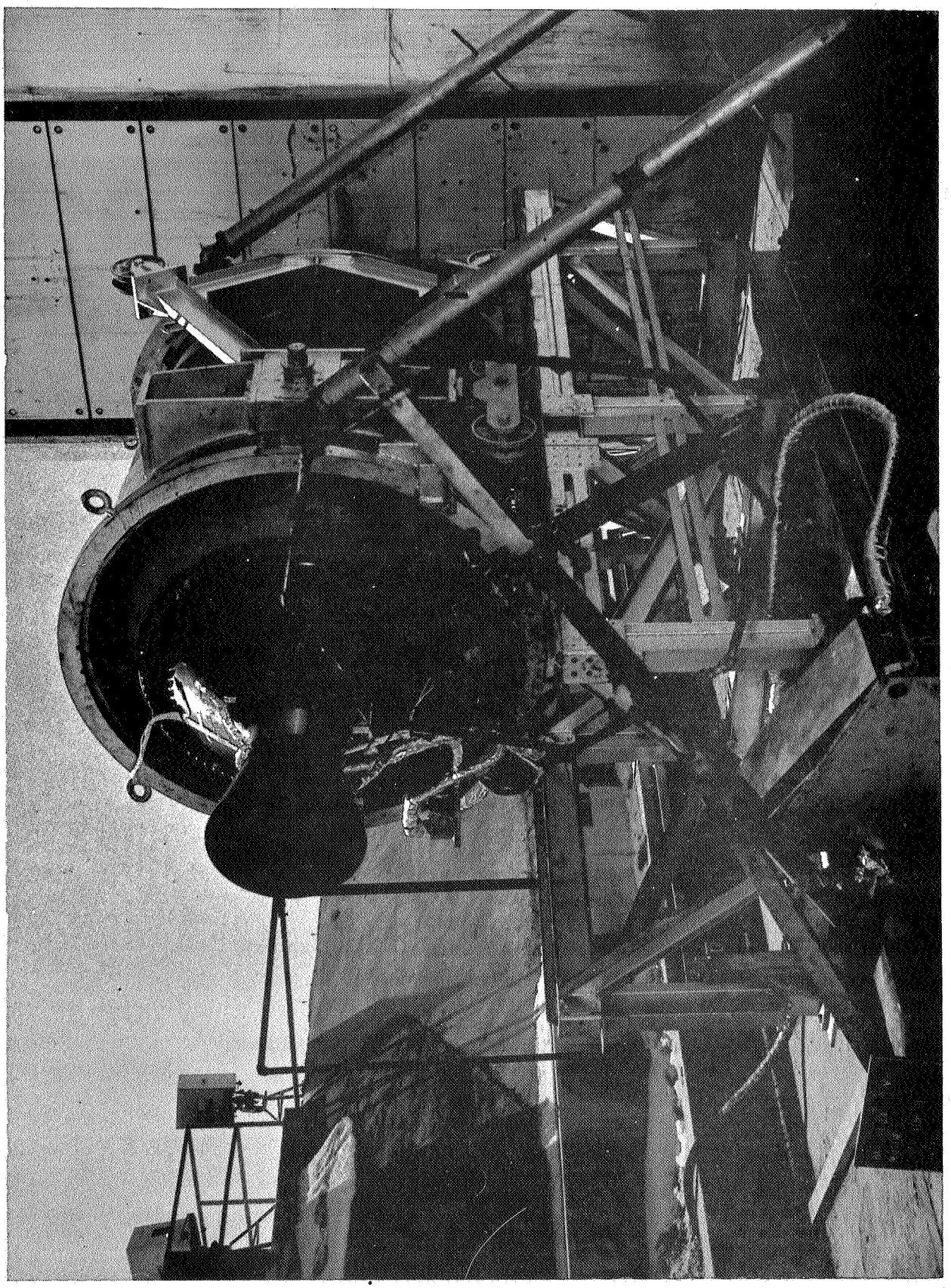

Figure 24 - 65-SS-2 Motor Setup Prior to Testing

GLOSSARY

The following terms are defined to obviate misinterpretation:

1. Action Time. Action time is defined as the interval from 75 percent of maximum pressure during rise to 10 percent of maximum pressure during tailoff.

2. Maximum Expected Operating Pressure (MEOP). MEOP is defined as that chamber pressure which may be expected when utilizing a 3-sigma variation in propellant burn rate at maximum operating temperature with consideration given to erosive burning conditions.

3. Outside Diameter of Case. The outside diameter of the case is defined as the diameter of the cylindrical portion of the case.

4. Port-to-Throat Ratio. The port-to-throat ratio is defined as the ratio between the initial port area of the grain to the initial nozzle throat area.

5. Specific Impulse. Specific impulse is defined as the total impulse divided by the calculated weight of propellant consumed during the action time.

6. Total Impulse. Total impulse is defined as the integrated thrust over the action time.

7. Web Action Time. Web action time is defined as the interval from 75 percent of maximum pressure during rise to the point of the pressure time trace which lies on the line bisecting the angle formed by the tangents on the trace prior to and immediately after the beginning of tailoff.

8. Propellant Web. Propellant web is defined as the radius of the propellant outside diameter minus the radius of the core outside diameter.

9. Web Fraction. Web fraction is defined as the ratio of the radius of the propellant outside diameter minus the radius of the core outside diameter divided by the radius of the propellant outside diameter.

10. Propellant Sliver Loss. Propellant sliver loss is defined as the predicted weight of propellant contained in the motor at the time at which the propellant web is consumed in the motor cylindrical section divided by the total propellant weight loaded into the motor. This number multiplied by 100 is equal to the percent of propellant sliver loss.

FINAL REPORT DISTRIBUTION LIST

SOLID ROCKET TECHNOLOGY

NASA Lewis Research Center
21000 Brookpark Road
Cleveland, Ohio 44135
Attn: Contracting Officer
Mail Stop 500-313 (1)
Solid Rocket Technology Branch
Mail Stop 500-205 (8)
Technical Library
Mail Stop 60-3 (2)
Tech. Report Control Office
Mail Stop 5-5 (1)
W. E. Roberts
Mail Stop 3-17 (1)

National Aeronautics and
Space Administration
Washington, D. C. 20546
Attn: RPM/William Cohen (3)
RPS/Robert W. Ziem (1)
ATSS-AL/Technical Library (2)

NASA Western Support Office
150 Pico Boulevard
Santa Monica, California 90406
Attn: Eugene F. Wyszpolski (1)
Harry Williams (1)

NASA Ames Research Center
Moffett Field, California 94035
Attn: Technical Library (1)

NASA Langley Research Center
Langley Station
Hampton, Virginia 23365
Attn: Robert L. Swain (1)
Technical Library (1)

NASA Goddard Space Flight Center
Greenbelt, Maryland 20771
Attn: Technical Library (1)

NASA Manned Spacecraft Center
2101 Webster Seabrook Road
Houston, Texas 77058
Attn: Technical Library (1)

NASA George C. Marshall Space
Flight Center
Redstone Arsenal
Huntsville, Alabama 35812
Attn: Technical Library (1)
R-P&VE-PA/K. Chandler (1)

Jet Propulsion Laboratory
California Institute of Technology
4800 Oak Grove Drive
Pasadena, California 91103
Attn: Richard Bailey (1)
Technical Library (1)

Scientific and Technical Information
Facility
NASA Representative
Post Office Box 33
College Park, Maryland 20740
Attn: CRT (1)

GOVERNMENT INSTALLATIONS

AF Space Systems Division
Air Force Unit Post Office
Los Angeles, California 90045 (1)
Attn: Col. E. Fink

AF Research and Technology Division
Bolling AFB, D. C. 20332
Attn: Dr. Leon Green, Jr. (1)

AF Rocket Propulsion Laboratory
Edwards AFB, California 93523
Attn: Norman Hirsch (1)
RPM/Col. R. Harned (2)

AF Materials Laboratory
Wright-Patterson AFB, Ohio 45433
Attn: MANC/D. Schmidt (1)
MAAE (1)

AF Ballistic Missile Division
Post Office Box 262
San Bernardino, California
Attn: WDSOT (1)

Structures Division
Wright Patterson AFB, Ohio 45433
Attn: FDT/R. F. Hoener (1)

Army Missile Command
Redstone Scientific Information Ctr.
Redstone Arsenal, Alabama 35809
Attn: Chief, Document Section (1)

Ballistic Research Laboratory
Aberdeen Proving Ground,
Maryland 21005
Attn: Technical Library (1)

Picatinny Arsenal
Dover, New Jersey 07801
Attn: Technical Library (1)

Navy Special Projects Office
Washington, D. C. 20360
Attn: H. Bernstein (1)

Naval Air Systems Command
Washington, D. C. 20360
Attn: AIR-330/Dr. O. H. Johnson (1)

Naval Propellant Plant
Indian Head, Maryland 20640
Attn: Technical Library (1)

Naval Ordnance Laboratory
White Oak
Silver Spring, Maryland 20910
Attn: Technical Library (1)

Naval Ordnance Test Station
China Lake, California 93557
Attn: Edward W. Price (1)
Technical Library (1)
C. J. Thelen (1)

Naval Research Laboratory
Washington, D. C. 20390
Attn: Technical Library (1)

Chemical Propulsion Information
Agency
Applied Physics Laboratory
8621 Georgia Avenue
Silver Spring, Maryland 20910 (1)

Defense Documentation Center
Cameron Station
5010 Duke Street
Alexandria, Virginia 22314 (1)

Defense Materials Information
Center
Battelle Memorial Institute
505 King Avenue
Columbus, Ohio 43201 (1)

Materials Advisory Board
National Academy of Science
2101 Constitution Avenue, N. W.
Washington, D. C. 20418
Attn: Capt. A. M. Blamphin (1)

Institute for Defense Analyses
1666 Connecticut Avenue, N. W.
Washington, D. C.
Attn: Technical Library (1)

Advanced Research Projects Agency
Pentagon, Room 3D154
Washington, D. C. 20301
Attn: Technical Information Office (1)

INDUSTRY CONTRACTORS

Aerojet-General Corporation
Post Office Box 1168
Solid Rocket Plant
Sacramento, California 94086
Attn: Dr. B. Simmons (1)
Technical Information Ctr. (1)

Aerojet-General Corporation
Post Office Box 296
Azusa, California 91702
Attn: Technical Library (1)

Aerospace Corporation
2400 East El Segundo Boulevard
El Segundo, California 90245
Attn: Technical Library (1)
Solid Motor Dev. Office (1)

Aerospace Corporation
Post Office Box 95085
Los Angeles, California 90045
Attn: Technical Library (1)

Atlantic Research Corporation
Shirley Highway at Edsall Road
Alexandria, Virginia 22314
Attn: Technical Library (1)

Battelle Memorial Library
505 King Avenue
Columbus, Ohio 43201
Attn: Edward Unger (1)

Boeing Company
Post Office Box 3999
Seattle, Washington 98124
Attn: Technical Library (1)

Chrysler Corporation
Space Division
Michoud Operations
New Orleans, Louisiana
Attn: Technical Library (1)

Douglas Missiles and Space Systems
Huntington Beach, California
Attn: T. J. Gordon (1)

Hercules Company
Allegany Ballistics Laboratory
Post Office Box 210
Cumberland, Maryland 21502
Attn: Technical Library (1)

Hercules Company
Bacchus Works
Post Office Box 98
Magna, Utah 84044
Attn: Technical Library (1)

Lockheed Missiles and Space Company
Post Office Box 504
Sunnyvale, California
Attn: Technical Library (1)

Lockheed Propulsion Company
Post Office Box 111
Redlands, California 92373
Attn: Bud White (1)

Martin Marietta Corporation
Baltimore Division
Baltimore, Maryland 21203
Attn: Technical Library (1)

Mathematical Sciences Corporation
278 Renook Way
Arcadia, California 91107
Attn: M. Fourney (1)

Philco Corporation
Aeronutronics Division
Ford Road
Newport Beach, California 92660
Attn: F. C. Price (1)

Rocketdyne
Solid Propulsion Operations
Post Office Box 548
McGregor, Texas
Attn: Technical Library (1)

Rocketdyne
6633 Canoga Avenue
Canoga Park, California 91304
Attn: Technical Library (1)

Rohm and Haas
Redstone Arsenal Research Division
Huntsville, Alabama 35807
Attn: Technical Library (1)

Rohr Corporation
Space Products Division
8200 Arlington Boulevard
Riverside, California
Attn: H. Clements (1)

Space Technology Laboratories, Inc.
5730 Arbor Vitae Street
Los Angeles, California 90045
Attn: Technical Library (1)

Thiokol Chemical Corporation
Wasatch Division
Brigham City, Utah 84302
Attn: B. L. Petty (1)

Thiokol Chemical Corporation
Elkton Division
Elkton, Maryland 21921
Attn: Technical Library (1)

Thiokol Chemical Corporation
Huntsville Division
Huntsville, Alabama 35807
Attn: Technical Library (1)

Thompson, Ramo, Wooldridge, Inc.
Structures Division
23444 Euclid Avenue
Cleveland, Ohio 44117
Attn: L. Russell (1)

United Technology Center
Post Office Box 358
Sunnyvale, California 94088
Attn: Technical Library (1)